

Numerical solution of dynamic equilibrium models under Poisson uncertainty*

Olaf Posch^(a) and Timo Trimborn^(b)

^(a)Hamburg University and CREATES, ^(b)University of Göttingen

February 2013

Abstract

We propose a simple and powerful numerical algorithm to compute the transition process in continuous-time dynamic equilibrium models with rare events. In this paper we transform the dynamic system of stochastic differential equations into a system of functional differential equations of the retarded type. We apply the Waveform Relaxation algorithm, i.e., we provide a guess of the policy function and solve the resulting system of (deterministic) ordinary differential equations by standard techniques. For parametric restrictions, analytical solutions to the stochastic growth model and a novel solution to Lucas' endogenous growth model under Poisson uncertainty are used to compute the exact numerical error. We show how (potential) catastrophic events such as rare natural disasters substantially affect the economic decisions of households.

JEL classification: C61, E21, O41

Keywords: Continuous-time DSGE, Poisson uncertainty, Waveform Relaxation

*Corresponding author: Olaf Posch (Email address: olaf.posch@uni-hamburg.de, Address: Hamburg University, Department of Economics, Von-Melle-Park 5, 20146 Hamburg, Germany. We thank Klaus Wälde, seminar and conference participants, and two anonymous referees for their comments. The first author appreciates financial support from the Center for Research in Econometric Analysis of Time Series, CREATES, funded by The Danish National Research Foundation.

1 Introduction

The stochastic growth model in continuous time has received extensive study in the macro literature (following Merton, 1975; Chang and Malliaris, 1987).¹ This benchmark economy gave rise to the development of advanced models for capturing the main features of aggregate fluctuations, often referred to as dynamic stochastic general equilibrium (DSGE) models. These models are the workhorse in dynamic macroeconomic theory. We use them to organize our thoughts, interpret empirical data and for policy recommendations.

The literature on DSGE models, however, has been surprisingly quiet on the effects of large economic shocks such as natural disasters and economic and/or financial crises. Most of the papers focus on small and frequent ‘business cycle shocks’. Therefore, departures from Normal uncertainty are largely unexplored. But the simple awareness of large and rare ‘Poisson jumps’ leads to an adjustment of households’ optimal consumption plans. One crucial difference to business cycle shocks is that an econometrician may not observe rare events for a longer period, and thus households might appear to be irrational.

In economic theory, however, we use Poisson events to model, e.g., natural disasters (Barro, 2006), technological improvements (Wälde, 1999, 2005),² exploration for exhaustible resources (Quyen, 1991), and financial market bubbles (Miller and Weller, 1990). Similarly, from an empirical perspective, beside anecdotal catastrophic events such as the 2004 Sumatra-Andoman earthquake and tsunami (South Asia), the 2005 Hurricane Katrina (USA) and the recent 2011 Sendai earthquake (Japan), rare disasters are found to have substantial asset pricing and welfare implications (Barro, 2009). Moreover, there is empirical evidence for rare Poisson jumps (positive and negative) in US macro data (Posch, 2009).

For most applications, economists need to rely on numerical methods to compute the solutions to their models. Thus the literature is making a huge effort in developing powerful computational methods (cf. Judd, 1992; Judd and Guu, 1997). Unfortunately, no rigorous treatment of how to solve dynamic equilibrium models under Poisson uncertainty numerically has been provided so far, and the effects of rare events on approximation errors are unknown.³

This paper proposes a simple and powerful method for determining the transition process in dynamic equilibrium models under Poisson uncertainty numerically. It turns out that local approximation techniques are not applicable and most global numerical recipes need to account for the specific nature of rare events. We show how to extend existing standard

¹The discrete-time one-sector stochastic neoclassical model was pioneered by Brock and Mirman (1972). The mathematical theory of the neoclassical growth model has its origin in Ramsey (1928).

²Rare events in the form of Poisson uncertainty also form the basis in quality ladder and matching models (Grossman and Helpman, 1991; Aghion and Howitt, 1992; Lentz and Mortensen, 2008).

³Generally most numerical methods are highly accurate locally (cf. Taylor and Uhlig, 1990; Christiano and Fisher, 2000; Schmitt-Grohé and Uribe, 2004; Aruoba, Fernández-Villaverde and Rubio-Ramírez, 2006).

45 algorithms when we allow for the possibility of rare events.

46 Our analysis builds on the continuous-time formulation of a stochastic neoclassical growth
47 model based on Merton (1975). We use the continuous-time formulation for two reasons.⁴
48 Firstly, we can easily compute stochastic differentials for transformations based on random
49 variables under Poisson uncertainty. Secondly, for reasonable parametric restrictions we can
50 solve the models by hand and obtain closed-form policy functions which can be used as
51 a point of reference and to compute the exact numerical error.⁵ From these benchmark
52 solutions our numerical method is used to explore broader parameterizations. Our idea is to
53 transform the system of stochastic differential equations (SDEs) into a system of functional
54 differential equations of the retarded type (Hale, 1977). We apply the Waveform Relaxation
55 algorithm, i.e., we provide a guess of the policy function and solve the resulting system of
56 (deterministic) ordinary differential equations (ODEs) by standard techniques.

57 This procedure is applicable to models which imply a dynamic system of controlled SDEs
58 under Poisson uncertainty. The controls are Markov controls in the form of policy functions
59 (cf. Sennewald, 2007). Although our method can also be applied to Normal uncertainty,
60 existing standard procedures can be used for this class of models (cf. Candler, 1999). We
61 therefore do not advocate the use of the Waveform Relaxation algorithm over alternative
62 approaches in all cases and applications. We aim at expanding the set of tools available to
63 researchers by showing how to solve dynamic economies under Poisson uncertainty.

64 We show that our solution method works. Although the suggested procedure computes
65 the policy functions for the complete state space — even for non-linear solutions — the
66 maximum (absolute) error compared to the exact solutions is very small. A strength of our
67 approach is that existing algorithms are easily extended to allow for Poisson uncertainty. We
68 illustrate our approach for two popular methods computing numerical solutions to dynamic
69 general equilibrium models, i.e., the backward integration (Brunner and Strulik, 2002) and
70 the Relaxation algorithm (Trimborn, Koch and Steger, 2008). From an economic point of
71 view, we find that (potential) large shocks affect optimal consumption and hours strategies.

72 The structure of the paper is as follows. In Section 2 of this paper, we describe the class
73 of models of interest. In Section 3, we describe the Waveform Relaxation method in detail
74 and discuss alternative approaches. In Section 4, we present two applications. The first is
75 the stochastic growth model with rare disasters. We choose parameterizations that allow
76 for analytical solutions to compute the numerical error. The second is the Lucas model
77 of endogenous growth including a novel analytical solution under Poisson uncertainty. We

⁴Continuous time models under uncertainty are widely used in economics (for a survey see Wälde, 2011), a continuous-time New Keynesian model is in Fernández-Villaverde, Posch and Rubio-Ramírez (2011).

⁵Analytical solutions for parametric restrictions are frequently used in macro models (Turnovsky, 1993, 2000; Corsetti, 1997; Wälde, 2005, 2011; Turnovsky and Smith, 2006; Posch, 2009).

78 conclude in Section 5.

79 **2 The macroeconomic theory**

80 This section introduces a broad class of economic models under Poisson uncertainty which
81 can be solved by means of Waveform Relaxation. Our algorithm (presented in Section 3.2)
82 can be used to study transitional dynamics in models under Poisson uncertainty. We show
83 how standard numerical techniques, which compute the optimal time paths of variables, can
84 be extended to allow for Poisson uncertainty, i.e., how they can be used to solve a system
85 of (stochastic) differential equations. A discussion of alternative approaches is provided in
86 Section 3.3. For this purpose, we develop our theoretical framework in Section 2.1, and then
87 present a simple procedure to obtain the (optimal) dynamic system in Section 2.2.

88 Our motivation stems from the rare disaster literature (Rietz, 1988; Barro, 2006, 2009).
89 Hence, our illustrations are mainly for rare events such as earthquakes or hurricanes which
90 remove a certain fraction of the capital stock. Obviously, our framework is not limited to this
91 particular class of models. For example, infrequent productivity increases are found in the
92 endogenous growth literature (Wälde, 2005). In any case, below we demonstrate that models
93 with rare (but potentially large) economic shocks are conceptionally different from models
94 with smaller shocks, e.g., ‘business cycle shocks’ resulting from Normal uncertainty. In a
95 nutshell, we show below that the Bellman equation for models under Poisson uncertainty is a
96 *functional* differential equation, while a partial differential equation is arising under Normal
97 uncertainty (cf. Sennewald, 2007; Wälde, 2011).

98 **2.1 The theoretical framework**

99 Consider the following infinite horizon stochastic control problem,

$$\max E \int_0^{\infty} e^{-\rho t} u(x_t, c_t) dt \quad s.t. \quad dx_t = f(x_t, c_t) dt + g(x_{t-}, c_{t-}) dN_t, \quad x_0 = x, \quad (1)$$

100 in which $x_t \in U_x$ denotes a vector of states from the state space $U_x \subseteq \mathbb{R}^{n_x}$, $c_t \in U_c$ denotes
101 a vector of controls from the control region $U_c \subseteq \mathbb{R}^{n_c}$, $u : U_x \times U_c \mapsto \mathbb{R}$, $f : U_x \times U_c \mapsto \mathbb{R}^{n_x}$
102 are vector functions which ensure concavity and boundedness, $g : U_x \times U_c \mapsto \mathbb{R}^{n_x \times n_x}$ is
103 an $n_x \times n_x$ matrix, and ρ is the rate of time preference. Let N_t denote the n_x vector of
104 (stochastically independent) Poisson processes with arrival rates $\lambda = (\lambda_1, \dots, \lambda_{n_x})^\top$.⁶ We
105 define $x_{t-} \equiv \lim_{s \rightarrow t} x_s$ for $s < t$ as the left-limit at time t such that x_{t-} is the value an
106 instant before a discontinuity (henceforth jump) and $x_t = x_{t-}$ for continuous paths.

⁶Though there is no conceptual difficulty in extending our analysis to models where the arrival rate is a function of the control and/or the state variable, $\lambda_t = \lambda(x_t, c_t)$, we consider constant arrival rates.

107 Economically, $u(x_t, c_t)$ specifies the (instantaneous) reward function, $f(x_t, c_t)$ denotes
 108 the drift function of the state variables and $g(x_t, c_t)$ is a matrix specifying the jump of state
 109 variables if a ‘disaster’ occurs. If such a rare event of the type i materializes, then $dN_{i,t} = 1$,
 110 which affects state variables through the i th column of the matrix $g(x_t, c_t)$.

111 2.2 Bellman’s principle and reduced form descriptions

Closely following Sennewald (2007), choosing an admissible control, $c \in U_c$ and defining $V(x)$ as the (optimal) value function, we obtain the *Bellman equation*

$$\rho V(x) = \max_{c \in U_c} \left\{ u(x, c) + \frac{1}{dt} E_0 dV(x) \right\},$$

112 which is a necessary condition for optimality. Using Itô’s formula (change of variables),

$$\begin{aligned} dV(x) &= V_x(x)^\top f(x, c)dt + \sum_{i=1}^{n_x} (V(x + g_i) - V(x)) dN_i \\ &\equiv V_x(x)^\top f(x, c)dt + v(x, c)^\top dN, \end{aligned}$$

113 in which V_x is the n_x vector of partial derivatives, g_i is the i th column of $g(x, c)$, and $v(x, c)$
 114 stacks the vector of jump terms of the value function corresponding to N . If we take the
 115 expectation of the integral form and use the martingale property, assuming that the above
 116 integrals exist (Sennewald, 2007, Theorem 2), we arrive at

$$E_0 dV(x) = V_x(x)^\top f(x, c)dt + v(x, c)^\top \lambda dt, \quad (2)$$

and the Bellman equation becomes

$$\rho V(x) = \max_{c \in U_c} \left\{ u(x, c) + V_x(x)^\top f(x, c) + v(x, c)^\top \lambda \right\}.$$

117 A neat result about the continuous-time formulation (compared to discrete-time models) is
 118 that the Bellman equation (2) is, in effect, a deterministic differential equation because the
 119 expectation operator disappears (Chang, 2004, p.118). The *first-order conditions* read

$$u_c(x, c) + f_c(x, c)^\top V_x(x) + \sum_{i=1}^{n_x} (\partial g_i(x, c) / \partial c)^\top V_x(x + g_i) \lambda_i = 0 \quad (3)$$

120 for any $t \in [0, \infty)$. The first two terms denote the first-order conditions as from deterministic
 121 control problems. In case the jump size is a function of the controls, we obtain additional
 122 terms represented by the third summand. These terms reflect the effect of the optimal
 123 control on the jump size of the states weighted by the probability of arrival. Note that the
 124 costate variable is evaluated at different values of the state variables.

From now on c denotes the optimal control variable. For the *evolution of the costate* we use the maximized Bellman equation,

$$\rho V(x) = u(x, c) + V_x(x)^\top f(x, c) + \sum_{i=1}^{n_x} (V(x + g_i) - V(x)) \lambda_i. \quad (4)$$

125 We make use of the envelope theorem to compute the costate,

$$\begin{aligned} \rho V_x(x) &= u_x(x, c) + f_x(x, c) V_x(x) + V_{xx}(x)^\top f(x, c) \\ &\quad + \sum_{i=1}^{n_x} ((I + \partial g_i(x, c)/\partial x)^\top V_x(x + g_i) - V_x(x)) \lambda_i, \end{aligned}$$

126 in which I denotes the n_x identity matrix. Collecting terms we obtain

$$\begin{aligned} \left[\left(\rho + \sum_{i=1}^{n_x} \lambda_i \right) I - f_x(x, c) \right] V_x(x) &= u_x(x, c) + V_{xx}(x)^\top f(x, c) \\ &\quad + \sum_{i=1}^{n_x} (I + \partial g_i(x, c)/\partial x)^\top V_x(x + g_i) \lambda_i. \end{aligned} \quad (5)$$

127 Using Itô's formula, the costate obeys

$$dV_x = V_{xx}(x)^\top f(x, c) dt + \sum_{i=1}^{n_x} (V_x(x + g_i) - V_x(x)) dN_i,$$

128 where inserting (5) yields the evolution of the costate variable

$$\begin{aligned} dV_x &= \left[\left(\rho + \sum_{i=1}^{n_x} \lambda_i \right) I - f_x(x, c) \right] V_x(x) dt - u_x(x, c) dt \\ &\quad - \sum_{i=1}^{n_x} (I + \partial g_i(x, c)/\partial x)^\top V_x(x + g_i) \lambda_i dt + \sum_{i=1}^{n_x} (V_x(x + g_i) - V_x(x)) dN_i. \end{aligned} \quad (6)$$

129 The evolution of the costate (6) consists mainly of three parts. Here, λ_i corresponds to
 130 the probability that a disaster of the type i occurs over the course of a period Δ , i.e., the
 131 probability of one jump during a period Δ is given by $e^{-\lambda_i \Delta} \lambda_i \Delta$. For $\lambda_i = 0$ ($\forall i = 1, \dots, n_x$)
 132 the costate evolves as in the standard deterministic model given by the first summand. The
 133 second part for $\lambda_i > 0$ illustrates the functional dependence of the costate not only on x , but
 134 also on the state variables to which the economy jumps in case a rare disaster of the type i
 135 occurs, $x + g_i$. In other words, households take into account that disasters may occur. The
 136 last part gives the actual jump terms in case of a disaster of the type i , in which $dN_i = 1$
 137 (N_i simply counts the number of arrivals of type i events).

138 For the general case, we solve the dynamic system (6) and the constraint in (1) together
 139 with the static condition (3) for the variables V_x , x and c .

140 For the case where $g(x, c) = g(x)$ does not depend on c , it is often possible to obtain
 141 *Euler equations* for consumption and eliminate the costate from the dynamic system. This
 142 yields a system of stochastic differential equations in x and c only. For this, we assume
 143 that the inverse function $c = h(V_x, x)$ for the optimality condition (3) exists and is strictly
 144 monotonic in both arguments. Then we may write the dynamic equilibrium system as

$$dx = f(x, c)dt + g(x)dN, \quad (7a)$$

$$dc = \frac{\partial h(V_x, x)}{\partial V_x} \left[dV_x - \sum_{i=1}^{n_x} (V_x(x + g_i(x)) - V_x(x)) dN_i \right] \\ + \frac{\partial h(V_x, x)}{\partial x} f(x, c)dt + \sum_{i=1}^{n_x} (h(V_x(x + g_i(x)), x + g_i(x)) - h(V_x(x), x)) dN_i, \quad (7b)$$

145 in which we insert dV_x from (6) and eliminate V_x using the static condition (3).

146 Further, the transversality condition is $\lim_{t \rightarrow \infty} e^{-\rho t} V(x) \geq 0$ for all admissible paths,
 147 where the equality holds for the optimal solution.

148 3 The numerical solution

149 This section transforms the reduced form (7) into a system of functional differential equations
 150 of the retarded type (RDEs). An extension to the more general case, where the costate
 151 variables cannot be eliminated, does not pose any conceptual difficulties.⁷ We apply the
 152 Waveform Relaxation algorithm, i.e., we provide a guess of the optimal policy function and
 153 solve the resulting systems of ODEs.

154 3.1 Description of the problem

155 The system of controlled stochastic differential equations (7) can be generalized to

$$dx_t = f(x_t, c_t) dt + g(x_{t-}) dN_t, \quad (8a)$$

$$dc_t = h(x_t, c_t, [c(x)]) dt + j(x_{t-}, c_{t-}, [c(x)]) dN_t, \quad (8b)$$

156 given initial states x_0 and transversality conditions. By the argument $[c(x)]$ we define the
 157 optimal solution or policy function, i.e., the optimal control as a function of a given state,
 158 $c = c(x)$. Here, a square bracket, $[\cdot]$, emphasizes the fact that the dependence of h and j on
 159 $c(x)$ is non-local, but on the whole policy function. The optimal solution $c(x)$ is of course *a*
 160 *priori* unknown. We assume that system (8) has a unique solution which only depends on
 161 the state variables and define the function $c(x) : U_x \subseteq \mathbb{R}^{n_x} \mapsto U_c \subseteq \mathbb{R}^{n_c}$, where U_x denotes

⁷Note that the proposed procedure handles algebraic equations in a straightforward way.

162 the state space and U_c the control region with n_x and n_c denoting the number of states and
163 controls. Similarly, we define the functions f, g, h and j as $f : U_x \times U_c \mapsto \mathbb{R}^{n_x}$, $g : U_x \mapsto \mathbb{R}^{n_x}$,
164 $h : U_x \times U_c \times C^k(U_x, U_c) \mapsto \mathbb{R}^{n_c}$, and $j : U_x \times U_c \times C^k(U_x, U_c) \mapsto \mathbb{R}^{n_c}$, respectively.⁸ All
165 functions are of class C^k , i.e., the partial derivatives of up to (and including) order k exist
166 and are continuous with k being sufficiently large.

167 Consumers' choice of control variables depends on the whole policy function $c(x)$, because
168 they consider the probability that a (Poisson) 'disaster' hits the economy. In this rare event,
169 the state variable x_t jumps by $g(x_{t-})$ and consumption adjusts accordingly. In normal times,
170 however, when no disaster occurs, consumers still consider the possibility that a disaster could
171 occur in the next instant of time for their optimal plans. In equation (6) this is illustrated
172 by the fact that the evolution of the costate depends on the current state *and* on the state
173 of the economy immediately after a disaster occurs. Equation (8b) accounts for this fact
174 by including the complete solution $c(x)$ on the right hand side. Hence, the more general
175 formulation of system (8) includes our system (7), and accounts exactly for this mechanism:
176 hypothetical 'after-disaster' states and controls influence today's decisions.

177 System (8) has to be augmented by boundary conditions for the beginning and the end
178 of the time horizon. Transversality conditions usually require (scale-adjusted) variables to
179 converge towards some interior steady states for $t \rightarrow \infty$, conditional on no jumps, $dN_t \equiv 0$.⁹
180 We denote steady-state values by $\{x^*, c^*\} \subseteq U_x \times U_c$. Generally, it is not sufficient to compute
181 the solution on some subdomain of U_x . The reason can be illustrated by the example of a
182 one-dimensional state space. If the domain is restricted to, e.g., $[x_0, x^*]$ the state could be
183 thrown back to an even smaller value than x_0 or jump to a value above x^* . For that reason,
184 the optimal control on $[x_0, x^*]$ depends on the optimal control for some $x_t < x_0$ and $x_t > x^*$.
185 To take this dependency into account the solution has to be computed on the domain U_x ,
186 which for macroeconomic problems typically is \mathbb{R}_+ . Extending this to an n_x -dimensional
187 state space the solution has to be calculated on the entire domain U_x .

188 3.2 The Waveform Relaxation algorithm

189 The crucial task for the numerical solution is to compute the policy function implied by the
190 (conditional) deterministic system, which means for $dN_t \equiv 0$,

$$dx_t = f(x_t, c_t) dt, \tag{9a}$$

$$dc_t = h(x_t, c_t, [c(x)]) dt. \tag{9b}$$

⁸For cases where one function, say $h = h(x_t, c_t, Z_t, [c(x)])$ is a function of a random variable, Z_t , in general our procedure requires conditioning, $Z_t = z$, such that $h = h(x_t, c_t, z, [c(x)]) \equiv \bar{h}(x_t, c_t, [c(x)])$.

⁹If no ambiguity arises, we use 'steady state' and 'conditional steady state' interchangeably.

191 In a second step, the stochastic paths are obtained by adding the Poisson process N_t , making
 192 use of the policy function $c_t = c(x_t)$. By construction, any solution to (9) solves the Bellman
 193 equation (4). The controls and the states follow the paths implied by the system (9) as long
 194 as no jump occurs (pathwise continuous). If a jump occurs at date t , the system adjusts
 195 according to j and g with $c_{t-} = c(x_{t-})$.

196 In the mathematical literature, the equations in system (9) are referred to as functional
 197 differential equations of the retarded type (cf. Hale, 1977; Kolmanovskii and Myshkis, 1999).
 198 A well-known special case of these equations are differential-difference equations (DDEs) in
 199 which the dynamic system exhibits a time delay (e.g., Boucekine, Germain, Licandro and
 200 Magnus, 1998, 2001; Asea, Zak 1999). In system (8), the jump term in case of a disaster is
 201 known in terms of controls and states, not in terms of time and, hence, the solution methods
 202 for DDEs are not suitable. This is why we apply a more general algorithm to solve functional
 203 differential equations. Our method is also suitable for solving systems of DDEs.

204 For calculating the policy function $c_t = c(x_t)$ we exploit the fact that numerous numerical
 205 methods are available to solve (9) *without* a dependency on the optimal solution,

$$dx_t = f(x_t, c_t) dt, \quad (10a)$$

$$dc_t = \tilde{h}(x_t, c_t) dt. \quad (10b)$$

206 The idea of Waveform Relaxation algorithms is as follows: by providing a guess of the
 207 policy function $c_0(x)$, system (9) reduces to (10), because the feedback of the solution path
 208 on dc_t is neglected.¹⁰ Now, problem (10) is a standard system of ODEs and can thus be
 209 solved by standard algorithms.¹¹ In general, the obtained solution $c_1(x)$ will be different
 210 from the initial guess $c_0(x)$. Hence, a solution of the original (deterministic) problem (9) is
 211 not found yet. In the next step the initial guess is updated to $c_1(x)$ and the loop is repeated.
 212 If the updated solution $c_i(x)$ is the same as the guess $c_{i-1}(x)$, a solution of the deterministic
 213 problem (9) is found (we summarize our Waveform Relaxation algorithm in Table 1).

214 More formally, we construct a fix-point iteration for the operator \mathcal{N} such that a function
 215 z is a fix point of this operator: $\mathcal{N}(z) = z$. The function z represents the desired solution,
 216 $z : \mathbb{R} \mapsto \mathbb{R}^{n_x+n_c}$. The operator \mathcal{N} is defined by a modification of problem (9). We start with
 217 a trial solution z_0 and iterate by evaluating \mathcal{N} , until $\|z_i - z_{i-1}\|$ is sufficiently small.

¹⁰Waveform Relaxation algorithms for initial value problems and appropriate error estimation are described in Feldstein, Iserles and Levin (1995), Bjørhus (1994) and Bartoszewski and Kwapisz (2001). Alternative procedures for solving system (9) are collocation methods as described in Bellen and Zennaro (2003).

¹¹For problems with one state variable, among others, these are the backward integration procedure (Brunner and Strulik, 2002) and the procedure of time elimination (Mulligan and Sala-i-Martin, 1991). For problems with multiple state variables we can use projection methods (e.g., Judd, 1992), the method of Mercenier and Michel (1994), and the Relaxation method (Trimborn et al., 2008).

Table 1: Summary of the Waveform Relaxation algorithm

| | | |
|--------|------------------|--|
| Step 1 | (Conditioning) | Construct the conditional deterministic system of RDEs (system 9). |
| Step 2 | (Initialization) | Provide an initial guess for the policy function. |
| Step 3 | (Solution) | Solve the resulting system of ODEs (system 10). |
| Step 4 | (Update) | Update the policy function. |
| Step 5 | (Iteration) | Repeat Step 3 and Step 4 until convergence. |

218 For defining the operator \mathcal{N} , we take a trial solution $c_0(x)$ as given. We define

$$dx_i = f(x_i, c_i) dt, \quad (11a)$$

$$dc_i = h(x_i, c_i, c_{i-1}(x)) dt, \quad (11b)$$

219 for each iteration $i = 1, \dots, n$. Thus, system (11) represent a system of ordinary differential
 220 equations which can be solved by the existing standard numerical methods.

221 For single-state problems ($n_x = 1$) we employ the backward integration method proposed
 222 by Brunner and Strulik (2002).¹² For a brief description of this method, recall that equations
 223 (11a) and (11b) represent a system of ODEs with an interior, computable stationary point.
 224 This point usually exhibits a saddle-point structure, i.e., a stable one-dimensional manifold
 225 (policy function) connecting the steady state to the origin, and an unstable one-dimensional
 226 manifold. Our task is to compute the stable manifold numerically, for which we exploit
 227 the saddle-point structure. By reversing time, the stable (unstable) manifold becomes an
 228 unstable (stable) manifold. Thus, by starting near the manifold, solution trajectories are
 229 attracted by the (optimal) policy function.

230 An important difference to standard methods in each iteration step is the evaluation of
 231 the function $c_i(x)$. Note that the solution of the previous iteration $c_{i-1}(x)$ is only available
 232 at certain points in the phase space. However, functions f and h of system (11) also need an
 233 evaluation of $c_{i-1}(x)$ at interior points. We employ a cubic spline interpolation of $c_{i-1}(x)$ to
 234 evaluate f and h . In order to control for the improvement in convergence, a suitable norm
 235 has to be chosen. We calculate the deviation of the policy function between two iterations
 236 on a mesh of points representing the whole state space U_x and employ the Euclidian norm
 237 $\|c_i(x_i) - c_{i-1}(x_i)\|$, where $x_i(1) < \dots < x_i(M)$ and M denotes the number of points on the
 238 mesh (M determines the accuracy of the solution).

239 For multiple-state problems ($n_x > 1$) we employ the Relaxation algorithm as described
 240 in Trimborn et al. (2008) to solve the deterministic system (11). This method can be applied
 241 to continuous-time deterministic problems with any number of state variables. The principle

¹²Note that backward iteration can be applied to any number of control variables, i.e., $n_c \geq 1$.

242 of relaxation is to construct a large set of non-linear equations, the solution of which repre-
243 sents the desired trajectory. This is achieved by a discretization of the involved differential
244 equations on a mesh of points in time. The set of differential equations is augmented by
245 algebraic equations representing equilibrium conditions or (static) no-arbitrage conditions at
246 each mesh point. Finally, equations representing the initial and final boundary conditions
247 are appended. The whole set of equations is solved simultaneously.

248 For multiple-state problems, we select starting values x_0 uniformly located in a rectangle
249 in the state space U_x and calculate transitional dynamics starting from each of these initial
250 values. The solutions give a good representation of the policy function. Again, the policy
251 function is only available on a mesh in the state space. Similar to the simulations with
252 a one-dimensional state space, we employ a cubic spline interpolation to obtain the policy
253 function at arbitrary interior points. Different from the procedure above, we use only the
254 initial value of each iteration for interpolation. This turns out to be a more robust approach,
255 presumably due to the evenly spaced grid one obtains in this case.

256 Similar to other procedures, complexity and computation time increases considerably
257 with the number of state variables, which is known as the ‘curse of dimensionality’. The
258 computational speed could be improved substantially, however, by using graphics processing
259 units (cf. Aldrich, Fernández-Villaverde, Gallant and Rubio-Ramírez, 2011). The idea is to
260 parallelize the algorithm and employ graphic processors to solve each independent step at
261 the same time. It is straightforward to parallelize the Waveform relaxation algorithm: each
262 of the transition paths starting at a particular initial position in the state space can be used
263 as one independent step and, hence, these paths can be calculated at the same time. Thus,
264 by parallelization, computational costs per iteration can be reduced considerably.

265 **3.3 Comparison to alternative approaches**

266 We briefly compare the Waveform Relaxation algorithm to alternative solution methods
267 which are frequently used in order to solve DGSE models. For a detailed description of these
268 methods see, for example, Judd (1998) and Marimon and Scott (1999).

269 **3.3.1 Local approximation methods**

270 Local approximation methods are widely applied in economics since they are known to solve
271 the stochastic models (under Normal uncertainty) efficiently. The effects of large economic
272 shocks on the approximation error, however, are largely unexplored. This is unfortunate since
273 the local approximation might be inaccurate far off the stationary state around which the
274 solution is approximated. Even without observing large economic shocks, as shown above,
275 households’ decisions near (or at) the steady state depend on the value of state variables off

276 the steady state, which again would lead to approximation errors since the solution technique
277 would incorrectly incorporate the effect of a potential disaster. The approximation error far
278 off the steady state thus propagates to the steady state region, which implies that local
279 methods might also approximate poorly the policy function around the steady state. This
280 property makes local numerical approximation techniques unattractive: a Poisson shock may
281 drive the economy far away from its steady state value (cf. Barro, 2006), i.e., it may do so
282 in regions where the accuracy is poor. For this reason, local methods are not suitable for
283 approximations of the policy functions in our models.

284 3.3.2 Global approximation techniques

285 A number of methods are customized to solve models with Normal uncertainty. Most of these
286 methods exploit the specific structure of the Bellman equation and thus are not suitable for
287 our problem. For example, Büttler (1995) and Candler (1999) apply finite differences to solve
288 the Bellman equation as a partial differential equation (PDE). However, finite differences
289 cannot be used to solve our functional differential equation. As illustrated before, the major
290 difficulty in using such methods is that the value function depends on the current state *and*
291 on the state of the economy immediately after a Poisson shock occurs.

292 We are aware of at least two global approaches capable of solving our problem at hand:
293 policy function (and value function) iteration and projection methods (spectral methods).
294 Both approaches solve for the policy function numerically using the standard contraction
295 mapping theorem which is independent from its particular functional form. One caveat
296 is that such methods may converge to a wrong solution since the unstable manifold also
297 solves the Bellman equation. Moreover, even for the standard stochastic growth model a
298 sophisticated initial guess for the policy function is needed in order to obtain the correct
299 solution and/or to achieve convergence (cf. Judd, 1992, p.431). Our approach is not subject
300 to those limitations. Since the Waveform Relaxation algorithm solves the system of ODEs
301 for the time path of variables instead of solving the Bellman equation, by construction, it
302 converges to the stable manifold.¹³ Hence, we do not encounter problems of convergence
303 towards the unstable manifold even when starting with an uninformative initial guess.

304 To summarize, the Waveform relaxation algorithm is a global and non-linear solution
305 method and scores with robustness and reliability. A detailed comparison to alternative
306 approaches along the lines of Taylor and Uhlig (1990) is on our research agenda.

¹³By solving for the time path of variables, the solution satisfies initial boundary conditions for time t_0 and final boundary conditions in the form of steady state values for time ∞ . Since our solution converges towards steady state values as $t \rightarrow \infty$, it characterizes the stable manifold.

4 Illustrative examples

The following examples are intended to illustrate potential economic applications in macro. To start with, we first consider the stochastic Ramsey problem with a single control and state variable, and then use a stochastic version of the Lucas model of endogenous growth mainly to illustrate the fact that multi-dimensional systems do not pose conceptual difficulties. In order to keep notation simple, we only consider problems faced by a benevolent planner, and use capital letters to denote variables in the planning problem which correspond to individual variables in the household's and firm's problems.

4.1 A neoclassical growth model with disasters

This section solves the stochastic neoclassical growth model under Poisson uncertainty which is motivated by the Barro-Rietz rare disaster hypothesis (Rietz, 1988; Barro, 2006).

Specification. Suppose that production takes the form of Cobb-Douglas, $Y_t = K_t^\alpha L^{1-\alpha}$, $0 < \alpha < 1$. Labor is supplied inelastically and capital can be accumulated according to

$$dK_t = (Y_t - C_t - \delta K_t) dt - \gamma K_t dN_t, \quad (K_0, N_0) \in \mathbb{R}_+^2, \quad 0 < \gamma < 1, \quad (12)$$

where N_t denotes the number of (natural) disasters up to time t , occasionally destroying γ percent of the capital stock K_t at an arrival rate $\lambda \geq 0$.¹⁴

The benevolent planner maximizes welfare by choosing the optimal path of consumption,

$$\max_{\{C_t\}_{t=0}^{\infty}} E \int_0^{\infty} e^{-\rho t} \frac{C_t^{1-\theta}}{1-\theta} dt \quad s.t. \quad (12). \quad (13)$$

Solution. From the Bellman principle, a necessary condition for optimality is

$$\rho V(K_0) = \max_{C_0 \in \mathbb{R}_+} \left\{ \frac{C_0^{1-\theta}}{1-\theta} + (K_0^\alpha L^{1-\alpha} - C_0 - \delta K_0) V_K(K_0) + (V(K_0 - \gamma K_0) - V(K_0)) \lambda \right\},$$

and the first-order condition corresponding to (3) reads

$$C_t^{-\theta} - V_K(K_t) = 0 \quad (14)$$

for any $t \in [0, \infty)$, making the control variable a function of the state variable, $C_t = C(K_t)$.

Hence, the problem (13) can be summarized as a system of controlled SDEs,

$$\begin{aligned} dK_t &= (K_t^\alpha L^{1-\alpha} - C_t - \delta K_t) dt - \gamma K_t dN_t, \\ dC_t &= (\alpha K_t^{\alpha-1} L^{1-\alpha} - \rho - \delta - \lambda + \lambda(1-\gamma)\tilde{C}(K_t)^{-\theta}) C_t / \theta dt - (1 - \tilde{C}(K_{t-})) C_t dN_t, \end{aligned}$$

in which we define $\tilde{C}(K_t) \equiv C((1-\gamma)K_t)/C(K_t)$, such that $1 - \tilde{C}(K_{t-})$ denotes the percentage drop of optimal consumption after a disaster.

¹⁴For a stochastic neoclassical growth model with elastic labor supply and the asset market implications of the Barro-Rietz rare disaster hypothesis, the interested reader is referred to Posch (2011).

328 4.1.1 Evaluation of the algorithm

329 We calculate numerical solutions for two benchmark calibrations. In both cases, an analytical
 330 representation of the policy function can be computed for plausible parameter restrictions.
 331 Therefore, we can compare numerical and analytical solutions and calculate computational
 332 errors to evaluate the performance of the Waveform Relaxation algorithm.¹⁵

333 Because the neoclassical growth model has one state variable, it is well suited for the
 334 backward integration procedure (cf. Brunner and Strulik, 2002). As explained above, by
 335 starting near the steady-state value K^* (the value towards which the economy converges if
 336 no disasters occur), the solution trajectories are attracted by the optimal policy function.¹⁶

337 Our first benchmark solution employs a plausible parameterization which allows for an
 338 analytical solution $(\alpha, \theta, \delta, \lambda, \gamma) = (0.5, 2.5, 0.05, 0.2, 0.1)$ similar to Posch (2009) and imposes
 339 $\rho = ((1 - \gamma)^{1-\alpha\theta} - 1)\lambda - (1 - \alpha\theta)\delta$ which gives $\rho = 0.0178$. Using this parametrization, the
 340 average time between two disasters is $1/\lambda = 5$ years, with each Poisson event destroying 10
 341 percent of the capital stock. For less frequent and/or smaller rare events, as e.g. for US
 342 data (with γ roughly 2.5 percent), our algorithm would improve performance since the true
 343 solution is closer to the deterministic guess. As shown in the appendix, consumers choose a
 344 constant saving rate $s \equiv 1/\theta$ and the policy function is $C_t = C(K_t) = (1 - s)L^{1-\alpha}K_t^\alpha$. Thus
 345 the optimal jump term is constant, $\tilde{C}(K_t) = (1 - \gamma)^\alpha$. Although technically a knife-edge
 346 solution, the policy functions for solutions around this parameter region are very similar.
 347 As shown in Figure 1, the deterministic policy function (for $\lambda = 0$ and/or $\gamma = 0$) and
 348 the stochastic policy function differ substantially for our calibration. This illustrates that
 349 (potential) rare events can have substantial effects on households' behavior.

350 Figures 2a and 2b show the absolute and relative error of the numerically obtained
 351 policy function compared to the analytical solution, respectively. Both plots indicate that
 352 the solution exhibits a high accuracy even for a large deviation from the steady state implied
 353 by economically large shocks. The absolute and relative errors compared to the true solution
 354 are below 10^{-8} within the most relevant interval between 0 and K^* . The maximum (absolute)
 355 errors are below 10^{-5} for values of capital of 150 percent of K^* , which is below the accuracy
 356 usually required for economic applications. Economically, this value denotes the error as a
 357 fraction of consumption at K_t : with a relative error of 10^{-5} , the consumer is making a \$1
 358 mistake for each \$10,000 spent (Aruoba et al., 2006, p.2499).

¹⁵The literature typically evaluates the performance using Euler equation residuals (see e.g. Judd, 1992). Santos (2000) shows that approximation errors of the policy function are of the same order of magnitude as the Euler equation residuals. Hence, we are able to compare our results with algorithms solving similar models (as in Aruoba, Fernández-Villaverde and Rubio-Ramírez, 2006; Dorofeenko, Lee and Salyer, 2010).

¹⁶For the backward integration procedure we deviate 10^{-12} in magnitude from the 'steady state' and we choose 10^{-14} as relative error tolerance for the Runge-Kutta procedure (cf. Brunner and Strulik, 2002).

359 Figures 2c and 2d show the absolute and relative change of the policy function, respec-
360 tively, compared to the previous iteration. It is apparent that both functions are of the same
361 shape and order of magnitude as the numerical errors compared to the analytical solution.
362 This shows that the change of the policy function between two iterations is an excellent ap-
363 proximation for measuring the numerical error of the solution. We make use of this striking
364 similarity to define our criterion function to gauge the accuracy of the numerical solution for
365 the general case where no analytical solution is available.

366 Our second benchmark solution requires the parametric restriction $\alpha = \theta$, which implies
367 a linear policy function, $C_t = C(K_t) = \phi K_t$.¹⁷ As shown in the appendix, the marginal
368 propensity to consume is $\phi = (\rho - ((1 - \gamma)^{1-\theta} - 1)\lambda - (\theta - 1)\delta)/\theta$. Since the policy function
369 is linear, the optimal jump term is constant, $\tilde{C}(K_t) = 1 - \gamma$. For ease of comparison, we
370 choose the same calibration for parameters as above, but a smaller value for the parameter
371 of relative risk aversion (or higher value for the intertemporal elasticity of substitution),
372 $\theta = 0.5$. As shown in Figure 3a both the deterministic policy function and stochastic policy
373 function are indeed linear in the capital stock. Once again, both policy functions differ
374 substantially. Figure 3b shows the optimal jump in consumption with respect to capital,
375 which is again independent of capital.

376 Figures 4a and 4b show the absolute and relative error of the numerically obtained policy
377 function compared to the analytical solution, respectively. In fact, the solution is obtained
378 already at the first iteration and exhibits a high accuracy of roughly 10^{-15} , close to the
379 machine's precision. The reason for immediate convergence and high accuracy lies in the
380 linearity of deterministic and stochastic policy functions: jump terms computed from a
381 linear policy function are independent from the policy function's slope and are thus already
382 correctly computed at the first iteration. Figures 4c and 4d show the absolute and relative
383 change of the policy function, respectively, compared to the previous iteration. Again both
384 measures are of similar shape and order of magnitude.

385 In order to show that the accuracy of the algorithm does not depend on the chosen
386 parameters, we conduct a sensitivity analysis with respect to the frequency of disasters, λ ,
387 and the percentage of capital that is destroyed by a disaster, γ . Parameter sets 1 and 4,
388 summarized in Table 2, reiterate our two benchmark calibrations. Parameter sets 2 and
389 5 assume that a higher proportion of the capital stock is destroyed if a disaster occurs
390 ($\gamma = 0.2$), but such disasters occur with a lower probability ($\lambda = 0.1$). Finally, parameter
391 sets 3 and 6 assume an even higher destruction rate ($\gamma = 0.4$) and a lower probability
392 ($\lambda = 0.05$) of disasters. The parameters are chosen such that an analytical solution is
393 available. For the parameter sets 1 to 3 we adjust the rate of time preference such that

¹⁷This solution is well established in macroeconomics (cf. Posch, 2009, and the references therein).

Table 2: Accuracy of the solution to the neoclassical growth model with disasters

| Parameter set ^{a)} | Number of iterations | absolute deviation (last iteration) $\ y_n - y_{n-1}\ $ | relative deviation (last iteration) $\ y_n/y_{n-1} - 1\ $ | absolute deviation (analytical solution) $\ y_n - y\ $ | relative deviation (analytical solution) $\ y_n/y - 1\ $ |
|-----------------------------|----------------------|--|--|---|---|
| 1 | 15 | $6.7 \cdot 10^{-6}$ | $5.2 \cdot 10^{-5}$ | $6.7 \cdot 10^{-6}$ | $1.2 \cdot 10^{-5}$ |
| 2 | 19 | $1.3 \cdot 10^{-6}$ | $1.9 \cdot 10^{-4}$ | $8.7 \cdot 10^{-7}$ | $1.3 \cdot 10^{-6}$ |
| 3 | 28 | $2.3 \cdot 10^{-9}$ | $6.5 \cdot 10^{-6}$ | $1.6 \cdot 10^{-9}$ | $9.0 \cdot 10^{-7}$ |
| 4 | 2 | $2.1 \cdot 10^{-13}$ | $1.1 \cdot 10^{-13}$ | $1.7 \cdot 10^{-13}$ | $1.0 \cdot 10^{-13}$ |
| 5 | 2 | $1.1 \cdot 10^{-13}$ | $7.5 \cdot 10^{-14}$ | $1.2 \cdot 10^{-13}$ | $8.0 \cdot 10^{-14}$ |
| 6 | 2 | $1.2 \cdot 10^{-13}$ | $1.6 \cdot 10^{-13}$ | $1.3 \cdot 10^{-13}$ | $1.3 \cdot 10^{-13}$ |

^{a)} Parameter sets used in the sensitivity analysis:

- 1: $(\alpha, \theta, \delta, \lambda, \gamma, \rho) = (0.5, 2.5, 0.05, \mathbf{0.2}, \mathbf{0.1}, 0.0178)$, 2: $(\alpha, \theta, \delta, \lambda, \gamma, \rho) = (0.5, 2.5, 0.05, \mathbf{0.1}, \mathbf{0.2}, 0.0182)$,
3: $(\alpha, \theta, \delta, \lambda, \gamma, \rho) = (0.5, 2.5, 0.05, \mathbf{0.05}, \mathbf{0.4}, 0.0193)$, 4: $(\alpha, \theta, \delta, \lambda, \gamma, \rho) = (0.5, 0.5, 0.05, \mathbf{0.2}, \mathbf{0.1}, 0.0178)$,
5: $(\alpha, \theta, \delta, \lambda, \gamma, \rho) = (0.5, 0.5, 0.05, \mathbf{0.1}, \mathbf{0.2}, 0.0178)$, 6: $(\alpha, \theta, \delta, \lambda, \gamma, \rho) = (0.5, 0.5, 0.05, \mathbf{0.05}, \mathbf{0.4}, 0.0178)$.

³⁹⁴ $\rho = ((1 - \gamma)^{1-\alpha\theta} - 1)\lambda - (1 - \alpha\theta)\delta$. For the parameter sets 4 to 6 we use $\alpha = \theta$. Our
³⁹⁵ results for parameter sets 1 to 3 show that the more severe disasters are (the more capital is
³⁹⁶ destroyed), the more iterations are necessary, while the accuracy of the algorithm remains
³⁹⁷ high. Results for parameter sets 4 to 6 show that convergence is indeed immediate and the
³⁹⁸ accuracy almost at the machine's precision for linear policy functions.

³⁹⁹ Our third illustration in Figure 5a shows both the deterministic and the stochastic policy
⁴⁰⁰ functions for the intermediate case of logarithmic preferences, $\theta = 1$, for which no analytical
⁴⁰¹ solution is known. As shown in Figure 5b the optimal jump term now indeed varies with
⁴⁰² the capital stock and the function $\tilde{C}(K_t)$ is decreasing in capital. As before, we iterate until
⁴⁰³ convergence, i.e., the change of the policy function between two iterations is sufficiently small
⁴⁰⁴ (cf. Figures 5a and 5b). Because no analytical benchmark solution is available, we now use
⁴⁰⁵ that both the absolute and relative change of the policy function between two iterations have
⁴⁰⁶ the same order of magnitude to conclude that the maximum (absolute) error is roughly 10^{-8}
⁴⁰⁷ within values for capital between 0 and 150 percent of K^* .

⁴⁰⁸ Finally, we should emphasize three main points: First, convergence does not depend on
⁴⁰⁹ parameter restrictions. The algorithm proves to be stable for a wide range of parameters.
⁴¹⁰ We restrict the presentation of results only due to lack of space. Second, computational
⁴¹¹ requirements are rather small. The solution of the model on a standard laptop requires
⁴¹² between some seconds and a few minutes. Third, our procedure can be implemented with
⁴¹³ an average ability in computational skills. While the numerical solution of the deterministic
⁴¹⁴ system is standard, the novel part of it is an interpolation routine based on the Waveform
⁴¹⁵ Relaxation idea. However, most software packages provide routines for (spline) interpolation.
⁴¹⁶ The Matlab codes and details of our implementation are summarized in a technical appendix,
⁴¹⁷ both are available on request.

418 4.1.2 The economic effects of rare disasters

419 Asking whether rare disasters lead to higher saving is equivalent to examining whether
420 more uncertainty raises or lowers the marginal propensity to consume. It is well established
421 that the intertemporal substitution effect depresses the marginal propensity to save for risk-
422 averse individuals. The optimum way to maintain the original utility level when uncertainty
423 increases is to consume more today (and thus avoid facing the disaster risk). In contrast,
424 the income effect is a precautionary savings effect, as higher uncertainty implies a higher
425 probability of low consumption tomorrow against which consumers will protect themselves
426 the more, by consuming less, the more averse they are to intertemporal fluctuations of
427 consumption (cf. Leland, 1968; Sandmo, 1970). By using a nonlinear production technology,
428 the neoclassical theory of growth under uncertainty offers a third channel through which
429 uncertainty has effects on the asymptotic distribution of capital (cf. Merton, 1975).

430 As shown in Weil (1990), the effect on optimal consumption (or saving) depends on
431 the magnitude of the intertemporal elasticity of substitution, $1/\theta$.¹⁸ Moreover, optimal
432 consumption depends on the degree of curvature of the production technology, α , since the
433 curvature of the policy function matters for effective risk aversion (cf. Posch, 2011). In case
434 the income effect is relatively small, $\theta < 1$, the presence of rare disasters tends towards
435 higher consumption (cf. Figure 3a). For the case where income and substitution effects
436 balance each other, $\theta = 1$, the only effect on consumption is due to the concave production
437 technology which depresses the marginal propensity to save (cf. Figure 5a), i.e., the mean
438 capital stock decreases. It is only when the intertemporal elasticity of substitution is small,
439 $\theta > 1$, the precautionary savings motive dominates the substitution effect and eventually
440 the effect of the nonlinear production technology, and savings increase (cf. Figure 1a).

441 4.2 Lucas' model of endogenous growth with disasters

442 This section uses the Waveform Relaxation algorithm to solve a stochastic version of the
443 Lucas (1988) endogenous growth model with two controls and two state variables. Motivated
444 by the rare disaster hypothesis, rare events – such as natural disasters – occasionally destroy
445 a fraction of the physical capital stock. Our solution method sheds light on the effects on
446 optimal consumption, human capital accumulation, and thus the balanced growth rate.

447 *Specification.* Consider a closed economy with competitive markets, with identical agents
448 and a Cobb-Douglas technology, $y_t = k_t^\alpha (u_t h_t)^{1-\alpha}$, where $0 < \alpha < 1$. Suppose at date t ,
449 workers (normalized to one) have skill level h_t and own the physical capital stock, k_t . A

¹⁸Weil (1990) shows that risk aversion, by determining the amplitude of the associated reduction in the certainty equivalent rate of return to saving, only affects the magnitude of the effects described above.

450 worker devotes u_t of his non-leisure time to current production, and the remaining $1 - u_t$ to
 451 human capital accumulation (improving skills). Hence, the effective aggregate hours devoted
 452 to production are $u_t h_t$. Denoting w_t as the hourly wage rate per unit of effective labor, the
 453 individual's labor income at skill h_t is $w_t h_t u_t$. Let the rental rate of physical capital be r_t .
 454 For simplicity there is no capital depreciation such that k_t evolves according to

$$dk_t = (r_t k_t + w_t u_t h_t - c_t) dt - \gamma k_t dN_t, \quad (16)$$

455 where N_t denotes the number of (natural) disasters up to time t , occasionally destroying
 456 $0 < \gamma < 1$ percent of the capital stock k_t at an arrival rate $\lambda \geq 0$.

To complete the model, the research effort $1 - u_t$ devoted to the accumulation of human capital must be linked to h_t . Suppose the technology relating the change of human capital dh_t to the level already attained and the effort devoted to acquiring more is

$$dh_t = (1 - u_t) \vartheta h_t dt. \quad (17)$$

457 According to (17), if no effort is devoted to human capital accumulation, $u_t = 1$, then non
 458 accumulates. If all effort is devoted to this purpose, $u_t = 0$, h_t grows at rate $\vartheta > 0$. In
 459 between these extremes, there are no diminishing returns to the stock h_t .

460 The resource allocation problem faced by the representative individual is to choose a time
 461 path for c_t and for u_t in $U_c \subseteq \mathbb{R}_+ \times [0, 1]$ such as to maximize expected life-time utility,

$$\max_{\{c_t, u_t\}_{t=0}^{\infty}} E_0 \int_0^{\infty} e^{-\rho t} \frac{c_t^{1-\theta}}{1-\theta} dt \quad s.t. \quad (16) \text{ and } (17), \quad (k_0, h_0, N_0) \in \mathbb{R}_+^3, \quad (18)$$

462 where $\theta > 0$ denotes constant relative risk aversion and ρ is the subjective time preference.

463 *Solution.* From the Bellman principle, choosing the controls $c_0, u_0 \in U_c$ requires the
 464 *Bellman equation* as a necessary condition for optimality,

$$\rho V(k_0, h_0) = \max_{c_0, u_0 \in U_c} \left\{ c_0^{1-\theta} / (1-\theta) + (r_0 k_0 + w_0 u_0 h_0 - c_0) V_k + (1 - u_0) \vartheta h_0 V_h \right. \\ \left. + (V((1 - \gamma)k_0, h_0) - V(k_0, h_0)) \lambda \right\}. \quad (19)$$

465 For any $t \in (0, \infty)$, the two *first-order conditions* corresponding to (3) are

$$c_t^{-\theta} - V_k = 0, \quad (20)$$

$$w_t h_t V_k - \vartheta h_t V_h = 0, \quad (21)$$

466 making the controls a function of the state variables, $c_t = c(k_t, h_t)$ and $u_t = u(k_t, h_t)$.

467 After some tedious algebra we obtain the Euler equations for consumption and hours.
 468 Together with initial and transversality conditions and constraints in (16) and (17), these

469 describe the equilibrium dynamics. We may summarize the reduced form dynamics by
 470 defining $\tilde{c}(k_t, h_t) \equiv c((1 - \gamma)k_t, h_t)/c(k_t, h_t)$ and $\tilde{u}(k_t, h_t) \equiv u((1 - \gamma)k_t, h_t)/u(k_t, h_t)$ as

$$dk_t = (r_t k_t + w_t u_t h_t - c_t) dt - \gamma k_{t-} dN_t, \quad (22a)$$

$$dh_t = (1 - u_t) \vartheta h_t dt, \quad (22b)$$

$$dc_t = \frac{r_t - \rho - \lambda + \tilde{c}(k_t, h_t)^{-\theta} (1 - \gamma) \lambda}{\theta} c_t dt + (\tilde{c}(k_{t-}, h_{t-}) - 1) c_{t-} dN_t, \quad (22c)$$

$$du_t = \left(\frac{1-\alpha}{\alpha} \vartheta + (\tilde{u}(k_t, h_t)^{-\alpha} - (1 - \gamma)^{1-\alpha}) (1 - \gamma)^\alpha \lambda \tilde{c}(k_t, h_t)^{-\theta} / \alpha - c_t / k_t + u_t \vartheta \right) u_t dt \\ + (\tilde{u}(k_t, h_t) - 1) u_{t-} dN_t, \quad (22d)$$

and the transversality condition reads (cf. Benhabib and Perli, 1994, p.117)

$$\lim_{t \rightarrow \infty} E_0 [V_k e^{-\rho t} [k_t - k_t^*] + V_h e^{-\rho t} [h_t - h_t^*]] \geq 0$$

471 for all admissible k_t and h_t , where k_t^* and h_t^* denote the optimal state values.

472 *Balanced growth.* From the reduced form system, we can derive the balanced growth
 473 rate of physical capital, human capital and consumption of the conditional deterministic
 474 system (conditioned on no disasters) as follows. First, we can neglect the stochastic integrals
 475 because for the case with no disasters $dN_t \equiv 0$. Second, similar to the deterministic model,
 476 the condition optimal research effort is constant, such that $du_t = 0$ must hold.

Now, for $du_t = 0$ research effort along the balanced growth path is implicitly given by
 $-\vartheta u^* = \frac{1-\alpha}{\alpha} \vartheta + (\tilde{u}^{-\alpha} - (1 - \gamma)^{1-\alpha}) (1 - \gamma)^\alpha \lambda \tilde{c}^{-\theta} / \alpha - c/k$, where $\tilde{u} \equiv \tilde{u}(k_t, h_t)$, $\tilde{c} \equiv \tilde{c}(k_t, h_t)$
 and $c/k \equiv c_t/k_t$ are constants. This property of the jump terms implies that asymptotically,
 $\tilde{c}(k_t, h_t) = \tilde{c}(k_t/h_t)$. Similarly, along this balanced growth path the other equations imply

$$g^k = r^*/\alpha - c/k, \quad g^h = (1 - u^*) \vartheta, \quad g^c = (r^* - \rho - \lambda + \tilde{c}^{-\theta} (1 - \gamma) \lambda) / \theta.$$

Since c_t/k_t is constant, c_t and k_t must grow at the same rate, $g^k = g^c$, which in turn implies
 $c/k = (r^* - \rho - \lambda + \tilde{c}^{-\theta} (1 - \gamma) \lambda) / \theta + r^*/\alpha$. Along this path we need r^* to be constant, which
 requires that k_t and h_t grow at the same rate, $g^k = g^h$. Hence, $r^*/\alpha - c/k = (1 - u^*) \vartheta$. This
 pins down the interest rate $r^* = \vartheta + (\tilde{u}^{-\alpha} - (1 - \gamma)^{1-\alpha}) \tilde{c}^{-\theta} (1 - \gamma)^\alpha \lambda$. Hence, the balanced
 growth rate of the *conditional* deterministic system is

$$g \equiv (\vartheta - \rho - \lambda + (1 - \gamma)^\alpha \tilde{u}^{-\alpha} \tilde{c}^{-\theta} \lambda) / \theta, \quad (23)$$

477 which finally implies the consumption-to-capital ratio

$$c/k = (\vartheta + (\tilde{u}^{-\alpha} - (1 - \gamma)^{1-\alpha}) \tilde{c}^{-\theta} (1 - \gamma)^\alpha \lambda - \rho - \lambda + \tilde{c}^{-\theta} (1 - \gamma) \lambda) / \theta \\ + (\vartheta + (\tilde{u}^{-\alpha} - (1 - \gamma)^{1-\alpha}) \tilde{c}^{-\theta} (1 - \gamma)^\alpha \lambda) / \alpha.$$

478 The growing variables of the reduced-form system c_t , h_t , and k_t in (22) need to be scaled
 479 such that they approach some stationary steady-state values (scale-adjustment).

480 *Scale-adjusted dynamics.* In what follows, we simply subtract the endogenous balanced
 481 growth rate (23) from the reduced-form system in instantaneous growth rates to obtain
 482 scale-adjusted variables. The scale-adjusted system (conditioned on no disasters) reads

$$d \ln k_t = (r_t + w_t u_t h_t / k_t - c_t / k_t - g) dt, \quad (24a)$$

$$d \ln h_t = (\vartheta - u_t \vartheta - g) dt, \quad (24b)$$

$$d \ln c_t = ((r_t - \rho - \lambda + \tilde{c}(k_t, h_t)^{-\theta} (1 - \gamma) \lambda) / \theta - g) dt, \quad (24c)$$

$$\begin{aligned} du_t &= \left(\frac{1-\alpha}{\alpha} \vartheta + (\tilde{u}(k_t, h_t)^{-\alpha} - (1-\gamma)^{1-\alpha}) (1-\gamma)^\alpha \lambda \tilde{c}(k_t, h_t)^{-\theta} / \alpha - c_t / k_t \right) u_t dt \\ &\quad + \vartheta u_t^2 dt, \end{aligned} \quad (24d)$$

483 where g follows iteratively from (23).

484 Note that in general it is not possible to compute the steady state levels in terms of
 485 variables k^* , h^* , c^* , and u^* from system (24). We presume that the stochastic model inherits
 486 this characteristic from its deterministic counterpart, which exhibits a ray of steady states,
 487 i.e., a center manifold of stationary equilibria (cf. Lucas, 1988; Caballé and Santos, 1993).
 488 Each point on this ray differs with respect to the level of physical and human capital and,
 489 hence, consumption the economy can generate. The particular stationary equilibrium, to
 490 which the economy finally converges is determined by the initial values of physical and human
 491 capital. Since in general the functions \tilde{c} and \tilde{u} are not known for the stochastic counterpart
 492 of the model, we are not able to prove this property for the general case. However, for the
 493 parametric restriction $\alpha = \theta$ we obtain a closed-form solution and indeed provide a proof
 494 of this property below. Moreover, our numerical results confirm that the stochastic model
 495 indeed exhibits a ray of steady states. A ‘steady-state’ value in the stochastic setup again
 496 refers to the value the economy converges if no disasters occur.

497 We are now prepared to solve this (scale-adjusted) system using the Relaxation algorithm
 498 together with the Waveform relaxation idea.

499 4.2.1 Evaluation of the algorithm

500 We calculate numerical solutions for the Lucas model employing a benchmark calibration for
 501 which an analytical solution is available. Again, we compare the numerical and analytical
 502 solutions to evaluate the algorithm’s accuracy. Moreover, we calculate numerical solutions
 503 for a second calibration for which no analytical solution is available.

504 Because this model has two state variables, we choose the Relaxation algorithm to solve
 505 system (10) (cf. Trimborn et al., 2008). As already mentioned this algorithm is capable of

506 solving deterministic systems with multiple state variables. Moreover, the algorithm can
 507 also solve models that exhibit a center manifold of stationary equilibria. Since the method
 508 calculates the solution path as a whole, the particular conditional steady state to which the
 509 economy converges is determined numerically.

510 Our benchmark solution uses the calibration $(\alpha, \vartheta, \lambda, \gamma, \rho) = (0.75, 0.075, 0.2, 0.1, 0.03)$
 511 and the parametric restriction $\theta = \alpha$. As shown in the appendix, in this case consumers
 512 optimally choose constant hours, $u_t = u = (\rho - (1 - \theta)\vartheta)/(\alpha\vartheta)$, and optimal consumption
 513 does not depend on human capital and is linear in physical capital, $c_t = c(k_t, h_t) = \varphi k_t$.
 514 $\varphi = (\rho - ((1 - \gamma)^{1-\theta} - 1)\lambda)/\theta$ denotes the marginal propensity to consume with respect to
 515 physical capital. Since the policy function is linear in physical capital, the optimal jump
 516 terms are constant, $\tilde{c}(k_t, h_t) = 1 - \gamma$ and trivially $\tilde{u}(k_t, h_t) = 1$. Observe that this solution is
 517 very similar to the neoclassical growth model, though the growth rate is endogenous. From
 518 (23) we find that for $\alpha = \theta$, the balanced growth rate (in normal times, after the transition)
 519 is not affected by the presence of rare events, $g = (\vartheta - \rho)/\theta$. Below we compare our numerical
 520 solution obtained by the Waveform Relaxation algorithm with the analytical solution.

521 Figures 7a and 7b, respectively, show the optimal level of consumption and the optimal
 522 jump in consumption with respect to physical capital and human capital. Note that the
 523 optimal jump in consumption is independent of both physical capital and human capital.
 524 Similar to the neoclassical growth model, we find that the deterministic policy function for
 525 consumption (for $\lambda = 0$ and/or $\gamma = 0$) and the stochastic counterpart differ substantially.
 526 Moreover, the center manifold of stationary equilibria of (scale-adjusted) values for human
 527 capital and physical capital is different from the deterministic model.

528 Figures 8a and 8b show the absolute and relative error of consumption for the computed
 529 mesh grid of physical and human capital. Given the nature of the problem, the (absolute)
 530 errors are extremely small, not exceeding 10^{-8} in magnitude. As explained above, this level
 531 of accuracy is higher than what is usually required for most economic applications. Figures
 532 8c and 8d show the absolute and relative change in the policy function for consumption,
 533 respectively, compared to the previous iteration. It is apparent that both functions are of
 534 the same shape and order of magnitude as the numerical errors compared to the analytical
 535 solution, which helps us to gauge the numerical error of the solution in the general case.

536 Similarly to the case of consumption, Figures 9a and 9b show the optimal level of hours
 537 worked and the optimal jump with respect to physical capital and human capital. Hours
 538 are independent of capital goods along the transition and, hence, do not adjust in case of a
 539 Poisson jump. Figures 10a and 10b show the absolute and relative error of hours worked,
 540 whereas the absolute and relative change in the policy function for hours compared to the
 541 previous iteration are shown in Figures 10c and 10d, respectively. Again, the maximum

542 (absolute) errors are very small and do not exceed 10^{-6} .

543 As an illustration for a case where closed-form solutions are not available, we compare our
544 benchmark solution to the case of logarithmic preferences, $\theta = 1$. Figures 11 and 13 show the
545 optimal policy functions for consumption and hours and the optimal jump in consumption
546 and hours, respectively. We find that the optimal levels and their jump terms now depend
547 on the level of physical capital and human capital. While the level of optimal consumption
548 is increasing in both capital goods, hours are increasing in human capital but decreasing
549 in physical capital. Hence, countries with an abundant supply of human capital but scarce
550 supply of physical capital tend to supply the most hours to production.

551 Again we would like to emphasize that we are able to calculate policy functions not only
552 for the parametric restrictions presented above, but for a wider range of parameter values.
553 However, the algorithm is not as stable as for the one-dimensional case and is less precise
554 mainly due to interpolation problems. Eventually, for extreme combination of parameter
555 values, problems of convergence might occur, or at least the procedure needs refinement with
556 respect to the chosen mesh and/or interpolation method. Since our main objective is to show
557 that multiple state variables do not pose conceptual problems for our solution method, we
558 leave this work for future research. The Matlab codes and details of our implementation are
559 summarized in a technical appendix, both available on request.

560 **4.2.2 The economic effects of rare disasters**

561 The Lucas model of endogenous growth has several channels through which uncertainty
562 enters in the economic decisions, and thus optimal plans will be affected when consumers
563 face more uncertainty. First, uncertainty will affect the consumption/saving decision as in the
564 neoclassical growth model. Second, uncertainty will enter the optimal allocation problem
565 of hours devoted to production and human capital accumulation. Finally, their optimal
566 behavior takes account of the effect on the (conditional) balanced growth path.

567 As shown in Figures 7a and 11a, the level of (scale-adjusted) consumption increases
568 for both calibrations, thus the dominating channel is the intertemporal substitution effect,
569 i.e., to consume more today (and thus avoid facing the disaster risk). In other words, the
570 intertemporal elasticity of substitution is sufficiently elastic to compensate the precautionary
571 savings effect. This is in line with the result from the neoclassical growth model.

572 In this model consumption is no longer the only way to accommodate the presence of risk.
573 From Figure 13a, for the case of logarithmic preferences with $\theta = 1$, we find that optimal
574 hours decrease due to the presence of rare disasters (a level shift). Intuitively, consumers
575 prefer to invest more in human capital accumulation which — in contrast to the physical
576 capital good — is not subject to disaster risk. Though it seems an intuitive response from

577 an asset pricing perspective, we find that this result cannot be generalized. As from Figure
578 9a, optimal hours are independent of the disaster risk. Supplying less hours for production
579 also has an income effect, which in the case of $\alpha = \theta$ exactly offsets the previous effect.
580 This example illustrates that it is important to study the effects of uncertainty within a
581 dynamic stochastic general equilibrium (DSGE) model, in order to avoid missing potentially
582 important feedback mechanisms when focusing on partial equilibrium effects only.

583 As from (23), the balanced growth rate (in normal times, after the transition) depends
584 on the optimal jump terms for both consumption and hours. In our numerical solution for
585 $\theta = 1$, the balanced growth rate of the deterministic system of $(\vartheta - \rho)/\theta = 4.5\%$ increases
586 by roughly 0.2 percentage points to $g = 4.7\%$ due to the presence of rare disasters. An
587 intuitive explanation of this effect is indeed the shift of optimal hours supplied to human
588 capital accumulation, and thus implying a higher growth rate in times without disasters.

589 **5 Conclusion**

590 In this paper we propose a simple and powerful method for determining the transitional
591 dynamics in continuous-time DSGE models under Poisson uncertainty. Our contribution is
592 to show how existing algorithms can be extended with an additional layer when we allow for
593 the possibility of rare events in the form of Poisson uncertainty.

594 We illustrate the algorithm by computing the stochastic neoclassical growth model and a
595 stochastic version of the Lucas model motivated by the Barro-Rietz rare disaster hypothesis.
596 We use analytical solutions for plausible parametric restrictions as a benchmark in order
597 to address the numerical accuracy. We find that even for non-linear policy functions, the
598 numerical error is extremely small.

599 From an economic perspective, we show that the simple awareness of the possibility of
600 infrequent large economic shocks affects optimal decisions and thus economic growth. The
601 effect is economically important and thus needs to be explored in future research.

602 An interesting extension of this paper would be to allow for Normal-Poisson uncertainty.
603 In fact, the idea of Waveform Relaxation is not limited to the class of models under Poisson
604 uncertainty. For models under Normal uncertainty, the Bellman equation reduces to a partial
605 differential equation, which is a specific type of a *functional* differential equation. Studying
606 the numerical properties of these models is part of our research agenda.

607 **References**

608 Aghion, P. and P. Howitt, “A model of growth through creative destruction,” *Econometrica*,

- 1992, *60* (2), 323–351.
- Aldrich, Eric M., Jesús Fernández-Villaverde, A. Ronald Gallant, and Juan F. Rubio-Ramírez, “Tapping the supercomputer under your desk: Solving dynamic equilibrium models with graphics processors,” *J. Econ. Dynam. Control*, 2011, *35*, 386–393.
- Aruoba, S. Boragan, Jesús Fernández-Villaverde, and Juan F. Rubio-Ramírez, “Comparing solution methods for dynamic equilibrium economies,” *J. Econ. Dynam. Control*, 2006, *30*, 2477–2508.
- Asea, Patrick K. and Paul J. Zak, “Time-to-build and cycles,” *J. Econ. Dynam. Control*, 1999, *23*, 1155–1175.
- Barro, Robert J., “Rare disasters and asset markets in the twentieth century,” *Quart. J. Econ.*, 2006, pp. 823–866.
- , “Rare disasters, asset prices, and welfare costs,” *Amer. Econ. Rev.*, 2009, *99* (1), 243–264.
- Bartoszewski, Z. and M. Kwapisz, “On error estimates for Waveform Relaxation methods for delay-differential equations,” *SIAM Journal on Numerical Analysis*, 2001, *38* (2), 639–659.
- Bellen, A. and M. Zennaro, *Numerical Methods for Delay Differential Equations*, Oxford: Oxford Science Publications, 2003.
- Benhabib, Jess and Roberto Perli, “Uniqueness and Indeterminacy: On the Dynamics of Endogenous Growth,” *J. Econ. Theory*, 1994, *63*, 113–142.
- Bjørhus, M., “On Dynamic Iterations for Delay Differential Equations,” *BIT*, 1994.
- Boucekkine, Raouf, Marc Germain, Omar Licandro, and Alphonse Magnus, “Creative destruction, investment volatility, and the average age of capital,” *J. Econ. Growth*, 1998, *3*, 361–384.
- , —, —, and —, “Numerical solution by iterative methods of a class of vintage capital models,” *J. Econ. Dynam. Control*, 2001, *25*, 655–669.
- Brock, William A. and Leonard J. Mirman, “Optimal Economic Growth And Uncertainty: The Discounted Case,” *J. Econ. Theory*, 1972, *4*, 479–513.
- Brunner, M. and H. Strulik, “Solution of Perfect Foresight Saddlepoint Problems: A Simple Method and Applications,” *J. Econ. Dynam. Control*, 2002, *26*, 737–753.

- 637 Büttler, Hans-Jürg, “Evaluation of Callable Bonds: Finite Difference Methods, Stability and
638 Accuracy,” *Economic J.*, 1995, 105 (429), 374–384.
- 639 Caballé, Jordi and Manuel S. Santos, “On Endogenous Growth with Physical and Human
640 Capital,” *J. Polit. Economy*, 1993, 101 (6), 1042–1067.
- 641 Candler, G.V., *Finite-difference methods for continuous-time dynamic programming*, in
642 R. Marimon and A. Scott (Eds.): *Computational Methods for the Study of Dynamic*
643 *Economies*, Oxford Univ. Press, 1999.
- 644 Chang, Fwu-Ranq, “The Inverse Optimal Problem: A Dynamic Programming Approach,”
645 *Econometrica*, 1988, 56 (1), 147–172.
- 646 —, *Stochastic optimization in continuous time*, Cambridge Univ. Press, 2004.
- 647 — and A. G. Malliaris, “Asymptotic Growth under Uncertainty: Existence and Uniqueness,”
648 *Rev. Econ. Stud.*, 1987, 54 (1), 169–174.
- 649 Christiano, Lawrence J. and Jonas D. M. Fisher, “Algorithms for solving dynamic models
650 with occasionally binding constraints,” *J. Econ. Dynam. Control*, 2000, 24, 1179–1232.
- 651 Corsetti, Giancarlo, “A portfolio approach to endogenous growth: equilibrium and optimal
652 policy,” *J. Econ. Dynam. Control*, 1997, 21, 1627–1644.
- 653 Dorofeenko, Victor, Gabriel Lee, and Kevin D. Salyer, “A new algorithm for solving dynamic
654 stochastic macroeconomic models,” *J. Econ. Dynam. Control*, 2010, 34, 388–403.
- 655 Feldstein, A., A. Iserles, and D. Levin, “Embedding of Delay Equations into an Infinite-
656 Dimensional ODE System,” *Journal of Differential Equations*, 1995, 117, 127–150.
- 657 Fernández-Villaverde, Jesús, Olaf Posch, and Juan F. Rubio-Ramírez, “Solving the New
658 Keynesian Model in Continuous Time,” *mimeo*, 2011.
- 659 Grossman, Gene M. and Elhanan Helpman, *Innovation and Growth in the Global Economy*,
660 Cambridge, Massachusetts: The MIT Press, 1991.
- 661 Hale, J., *Theory of Functional Differential Equations*, New York: Springer, 1977.
- 662 Judd, Kenneth L., “Projection methods for solving aggregate growth models,” *J. Econ.*
663 *Theory*, 1992, 58, 410–452.
- 664 —, *Numerical Methods in Economics*, MIT Press, 1998.

- 665 — and Sy-Ming Guu, “Asymptotic methods for aggregate growth models,” *J. Econ. Dynam.*
666 *Control*, 1997, *21*, 1025–1042.
- 667 Kolmanovskii, V. and A. Myshkis, *Introduction to the Theory and Applications of Functional*
668 *Differential Equations*, Boston: Kluwer Academic, 1999.
- 669 Leland, Hayne E., “Saving and Uncertainty: The Precautionary Demand for Saving,” *Quart.*
670 *J. Econ.*, 1968, *82* (3), 465–473.
- 671 Lentz, Rasmus and Dale T. Mortensen, “An empirical model of growth through production
672 innovation,” *Econometrica*, 2008, *76* (6), 1317–1373.
- 673 Lucas, Robert E. Jr., “On the Mechanics of Economic Development,” *J. Monet. Econ.*, 1988,
674 *22*, 3–42.
- 675 Marimon, Ramon and Andrew Scott, *Computational Methods for the Study of Dynamic*
676 *Economies*, Oxford Univ. Press, 1999.
- 677 Mercenier, J. and P. Michel, “Discrete-time finite horizon approximation of infinite horizon
678 optimization problems with steady-state invariance,” *Econometrica*, 1994, *62* (3), 635–656.
- 679 Merton, Robert C., “An asymptotic theory of growth under uncertainty,” *Rev. Econ. Stud.*,
680 1975, *42* (3), 375–393.
- 681 Miller, Marcus H. and Paul Weller, “Currency bubbles which affect fundamentals: A quali-
682 tative treatment,” *Economic J.*, 1990, *100* (400), 170–179.
- 683 Mulligan, C. and X. Sala-i-Martin, “A Note on the Time Elimination Method for Solving
684 Recursive Growth Models,” *NBER Technical Working Paper*, 1991, *116*.
- 685 Posch, Olaf, “Structural estimation of jump-diffusion processes in macroeconomics,” *J.*
686 *Econometrics*, 2009, *153* (2), 196–210.
- 687 —, “Risk premia in general equilibrium,” *J. Econ. Dynam. Control*, 2011, *35* (9), 1557–1576.
- 688 Quyen, N. V., “Exhaustible Resources: A Theory of Exploration,” *Rev. Econ. Stud.*, 1991,
689 *58* (4), 777–789.
- 690 Ramsey, Frank, “A Mathematical Theory of Saving,” *Econ. J.*, 1928, *38*, 543–559.
- 691 Rietz, Thomas A., “The equity risk premium: A solution,” *J. Monet. Econ.*, 1988, *22*,
692 117–131.

- 693 Ruiz-Tamarit, José Ramón, “The closed-form solution for a family of four-dimension non-
694 linear MHDS,” *J. Econ. Dynam. Control*, 2008, *32*, 1000–1014.
- 695 Sandmo, A., “The Effect of Uncertainty on Saving Decisions,” *Rev. Econ. Stud.*, 1970, *37*
696 (3), 353–360.
- 697 Santos, Manuel S., “Accuracy of Numerical Solutions Using the Euler Equation Residuals,”
698 *Econometrica*, 2000, *68* (6), 1377–1402.
- 699 Schmitt-Grohé, Stephanie and Martin Uribe, “Solving dynamic general equilibrium models
700 using a second-order approximation to the policy function,” *J. Econ. Dynam. Control*,
701 2004, *28*, 755–775.
- 702 Sennewald, Ken, “Controlled stochastic differential equations under Poisson uncertainty and
703 with unbounded utility,” *J. Econ. Dynam. Control*, 2007, *31* (4), 1106–1131.
- 704 Taylor, John B. and Harald Uhlig, “Solving nonlinear stochastic growth models: A compar-
705 ison of alternative solution methods,” *J. Bus. Econ. Statist.*, 1990, *8* (1), 1–17.
- 706 Trimborn, T., K.-J. Koch, and T. M. Steger, “Multi-Dimensional Transitional Dynamics: A
707 Simple Numerical Procedure,” *Macroecon. Dynam.*, 2008, *12* (3), 1–19.
- 708 Turnovsky, Stephen J., “Macroeconomic policies, growth, and welfare in a stochastic econ-
709 omy,” *Int. Econ. Rev.*, 1993, *34* (4), 953–981.
- 710 —, *Methods of Macroeconomic Dynamics*, Cambridge, Massachusetts: MIT Press, 2000.
- 711 — and William T. Smith, “Equilibrium consumption and precautionary savings in a stochas-
712 tically growing economy,” *J. Econ. Dynam. Control*, 2006, *30*, 243–278.
- 713 Weil, Philippe, “Nonexpected utility in macroeconomics,” *Quart. J. Econ.*, 1990, *105* (1),
714 29–42.
- 715 Wälde, Klaus, “A model of creative destruction with undiversifiable risk and optimising
716 households,” *Econ. J.*, 1999, *109*, 156–171.
- 717 —, “Endogenous growth cycles,” *Int. Econ. Rev.*, 2005, *46* (3), 867–894.
- 718 —, “Production technologies in stochastic continuous time models,” *J. Econ. Dynam. Con-
719 trol*, 2011, *35* (4), 616–622.

720 **A Analytical benchmark solutions**

721 **A.1 An analytical solution to the neoclassical growth model**

722 The idea is to provide a guess of the value function and derive conditions under which both
723 the first-order condition and the maximized Bellman equation hold (cf. Posch, 2009).

724 Suppose that

$$V(K_t) = \frac{\mathbb{C}_1 K_t^{1-\alpha\theta}}{1-\alpha\theta}. \quad (25)$$

725 From (14), optimal consumption per effective worker is a constant fraction of income,

$$C_t^{-\theta} = \mathbb{C}_1 K_t^{-\alpha\theta} \quad \Leftrightarrow \quad C_t = C(K_t) = \mathbb{C}_1^{-1/\theta} K_t^\alpha.$$

726 Now use the maximized Bellman equation together with CRRA utility $u(C_t) = C_t^{1-\theta}/(1-\theta)$
727 and insert the solution candidate,

$$\rho V(K_t) = \frac{C(K_t)^{1-\theta}}{1-\theta} + (K_t^\alpha L^{1-\alpha} - C(K_t) - \delta K_t) V_K + (V((1-\gamma)K_t) - V(K_t)) \lambda,$$

728 which is equivalent to

$$\begin{aligned} (\rho + \lambda) \frac{\mathbb{C}_1 K_t^{1-\alpha\theta}}{1-\alpha\theta} &= \frac{\mathbb{C}_1^{-\frac{1-\theta}{\theta}} K_t^{\alpha-\alpha\theta}}{1-\theta} + \left(K_t^\alpha L^{1-\alpha} - \mathbb{C}_1^{-1/\theta} K_t^\alpha - \delta K_t \right) \mathbb{C}_1 K_t^{-\alpha\theta} \\ &\quad + \frac{\mathbb{C}_1 K_t^{1-\alpha\theta}}{1-\alpha\theta} (1-\gamma)^{1-\alpha\theta} \lambda \\ \Leftrightarrow 0 &= \frac{\theta}{1-\theta} \mathbb{C}_1^{-\frac{1}{\theta}} + L^{1-\alpha} - (\rho + (1-\alpha\theta)\delta + \lambda - (1-\gamma)^{1-\alpha\theta} \lambda) \frac{K_t^{1-\alpha}}{1-\alpha\theta}. \end{aligned}$$

729 This equation has a solution for $\mathbb{C}_1^{-1/\theta} = (\theta-1)/\theta L^{1-\alpha}$ and

$$\rho = (1-\gamma)^{1-\alpha\theta} \lambda - \lambda - (1-\alpha\theta)\delta. \quad (26)$$

730 For reasonable parametric calibrations equation (26) is satisfied. Though being a special case,
731 a Keynesian consumption function could be an admissible policy function for the neoclassical
732 model (cf. also Chang, 1988). Its plausibility is an empirical question.

733 **A.2 An analytical solution to the Lucas model**

734 We start with an educated guess on the value function and derive conditions under which it
735 actually is the unique solution of the optimal stochastic control problem. Suppose that

$$V(k_t, h_t) = \frac{\mathbb{C}_1 k_t^{1-\theta} + \mathbb{C}_2 h_t^{1-\theta}}{1-\theta}. \quad (27)$$

From (20), we obtain that optimal consumption is a linear function in the capital stock

$$c_t^{-\theta} = \mathbb{C}_1 k_t^{-\theta} \quad \Rightarrow \quad c(k_t, h_t) = \mathbb{C}_1^{-\frac{1}{\theta}} k_t. \quad (28)$$

736 Similarly, from (21) we obtain the optimal share of hours allocated to production, u_t ,

$$w_t h_t \mathbb{C}_1 k_t^{-\theta} = \vartheta h_t \mathbb{C}_2 h_t^{-\theta} \quad \Leftrightarrow \quad u(k_t, h_t) = \left(\frac{\vartheta}{(1-\alpha)} \frac{\mathbb{C}_2}{\mathbb{C}_1} h_t^{\alpha-\theta} k_t^{\theta-\alpha} \right)^{-\frac{1}{\alpha}},$$

737 in which we use $w_t = (1-\alpha)k_t^\alpha(u_t h_t)^{-\alpha}$. Observe that for the parametric restriction $\alpha = \theta$,
738 optimal hours allocated to production becomes a constant,

$$\alpha = \theta \quad \Rightarrow \quad u(k_t, h_t) = \left(\frac{\vartheta}{(1-\alpha)} \frac{\mathbb{C}_2}{\mathbb{C}_1} \right)^{-\frac{1}{\alpha}}.$$

739 Using the maximized Bellman equation, we may write with $r_t = \alpha k_t^{\alpha-1} (u_t h_t)^{1-\alpha}$

$$\begin{aligned} \rho V(k_t, h_t) &= \frac{c(k_t, h_t)^{1-\theta}}{1-\theta} + (k_t^\alpha (u(k_t, h_t) h_t)^{1-\alpha} - c(k_t, h_t)) V_k + (1 - u(k_t, h_t)) \vartheta h_t V_h \\ &\quad + (V((1-\gamma)k_t, h_t) - V(k_t, h_t)) \lambda. \end{aligned}$$

740 Inserting the guess for the value function gives

$$\begin{aligned} (\rho + \lambda) \frac{\mathbb{C}_1 k_t^{1-\theta} + \mathbb{C}_2 h_t^{1-\theta}}{1-\theta} &= \frac{c(k_t, h_t)^{1-\theta}}{1-\theta} + (k_t^\alpha (u(k_t, h_t) h_t)^{1-\alpha} - c(k_t, h_t)) \mathbb{C}_1 k_t^{-\theta} \\ &\quad + (1 - u(k_t, h_t)) \vartheta h_t \mathbb{C}_2 h_t^{-\theta} + \frac{\mathbb{C}_1 (1-\gamma)^{1-\theta} k_t^{1-\theta} + \mathbb{C}_2 h_t^{1-\theta}}{1-\theta} \lambda. \end{aligned}$$

741 Now insert the policy function for consumption $c(k_t, h_t)$,

$$\begin{aligned} (\rho + \lambda) \frac{\mathbb{C}_1 k_t^{1-\theta} + \mathbb{C}_2 h_t^{1-\theta}}{1-\theta} &= \frac{\mathbb{C}_1^{-\frac{1-\theta}{\theta}} k_t^{1-\theta}}{1-\theta} + (k_t^\alpha (u(k_t, h_t) h_t)^{1-\alpha} - \mathbb{C}_1^{-\frac{1}{\theta}} k_t) \mathbb{C}_1 k_t^{-\theta} \\ &\quad + (1 - u(k_t, h_t)) \vartheta \mathbb{C}_2 h_t^{1-\theta} + \frac{\mathbb{C}_1 (1-\gamma)^{1-\theta} k_t^{1-\theta} + \mathbb{C}_2 h_t^{1-\theta}}{1-\theta} \lambda. \end{aligned}$$

742 Now, we employ the restriction $\theta = \alpha$ such that optimal hours are constant, $u(k_t, h_t) = u$,

$$\begin{aligned} (\rho + \lambda) \frac{\mathbb{C}_1 k_t^{1-\theta} + \mathbb{C}_2 h_t^{1-\theta}}{1-\theta} &= \frac{\mathbb{C}_1^{-\frac{1-\theta}{\theta}} k_t^{1-\theta}}{1-\theta} + (u^{1-\alpha} h_t^{1-\alpha} - \mathbb{C}_1^{-\frac{1}{\theta}} k_t^{1-\theta}) \mathbb{C}_1 \\ &\quad + (1 - u) \vartheta \mathbb{C}_2 h_t^{1-\theta} + \frac{\mathbb{C}_1 (1-\gamma)^{1-\theta} k_t^{1-\theta} + \mathbb{C}_2 h_t^{1-\theta}}{1-\theta} \lambda. \end{aligned}$$

743 Collecting terms, we obtain

$$\begin{aligned} &(\rho + \lambda - \theta \mathbb{C}_1^{-\frac{1}{\theta}} - (1-\gamma)^{1-\theta} \lambda) \mathbb{C}_1 k_t^{1-\theta} = \\ &((1-\theta) u^{1-\alpha} \mathbb{C}_1 + (1-\theta)(1-u) \vartheta \mathbb{C}_2 - (\rho + \lambda) \mathbb{C}_2 + \mathbb{C}_2 \lambda) h_t^{1-\theta}. \end{aligned}$$

744 Hence, the first constant is pinned down by $\mathbb{C}_1 = (\theta/(\rho + \lambda - (1 - \gamma)^{1-\theta}\lambda))^\theta$. Inserting u
745 finally pins down the second constant,

$$\begin{aligned} \rho\mathbb{C}_2 &= (1 - \theta)u^{1-\alpha}\mathbb{C}_1 + (1 - \theta)(1 - u)\vartheta\mathbb{C}_2 \\ \Leftrightarrow \frac{\rho - (1 - \theta)\vartheta}{(1 - \theta)\vartheta} &= \frac{\alpha}{1 - \alpha} \left(\frac{\vartheta}{(1 - \alpha)} \right)^{-\frac{1}{\alpha}} \mathbb{C}_1^{\frac{1}{\alpha}} \mathbb{C}_2^{-\frac{1}{\alpha}} \\ \Rightarrow \mathbb{C}_2 &= \left(\frac{\alpha\vartheta}{\rho - (1 - \theta)\vartheta} \right)^\alpha \frac{1 - \alpha}{\vartheta} \left(\frac{\theta}{\rho + \lambda - (1 - \gamma)^{1-\theta}\lambda} \right)^\theta. \end{aligned}$$

746 Observe that we solved *not only* for some balanced growth path, but for the whole transition
747 path for a parameter restriction. To summarize, for $\alpha = \theta$ we obtain

$$c(k_t, h_t) = c(k_t) = \frac{\rho + \lambda - (1 - \gamma)^{1-\theta}\lambda}{\theta} k_t, \quad (29)$$

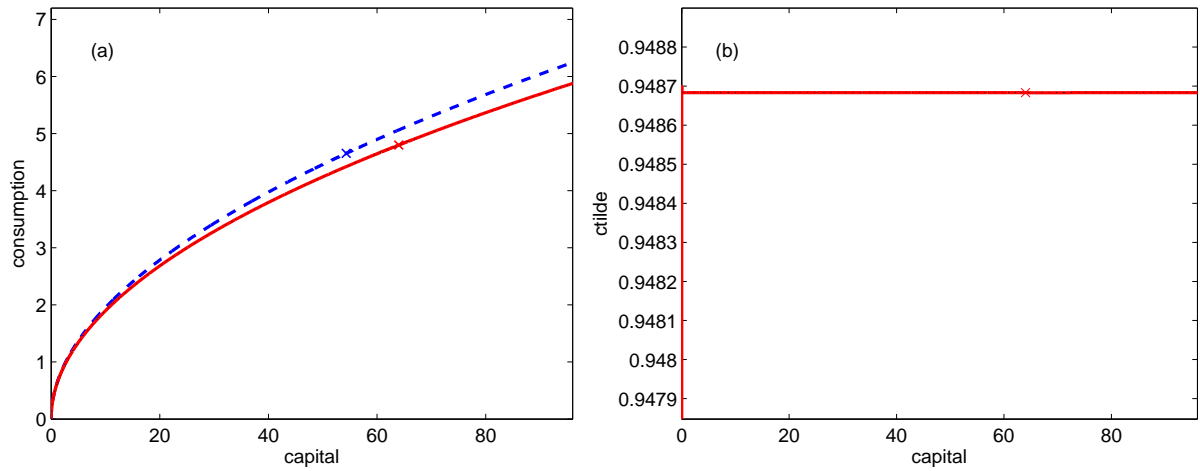
$$u(k_t, h_t) = u = \frac{\rho - (1 - \theta)\vartheta}{\alpha\vartheta}. \quad (30)$$

748 Hence, individuals prefer relatively more consumption (or less investment) but work the same
749 hours compared to the deterministic model for $\alpha = \theta$ (a similar condition for deterministic
750 Hamiltonian dynamic systems is in Ruiz-Tamarit, 2008). Note that the analytical solution
751 to the stochastic extension of the Lucas model is novel.

752 **B Figures**

753 **B.1 A neoclassical growth model with disasters**

Figure 1: Policy functions and optimal jump in the neoclassical growth model (i)



Notes: These figures show (a) the optimal policy functions: deterministic (dashed) vs. stochastic (solid) in the neoclassical growth model compared to the analytical benchmark solution (dotted), and (b) the optimal jump as a function of capital for the parameter set 1 from Table 2: $(\alpha, \theta, \delta, \lambda, \gamma, \rho) = (0.5, 2.5, 0.05, 0.2, 0.1, 0.0178)$, which implies a constant saving rate.

Figure 2: Absolute and relative error compared to the analytical benchmark solution and to the policy function of the last iteration

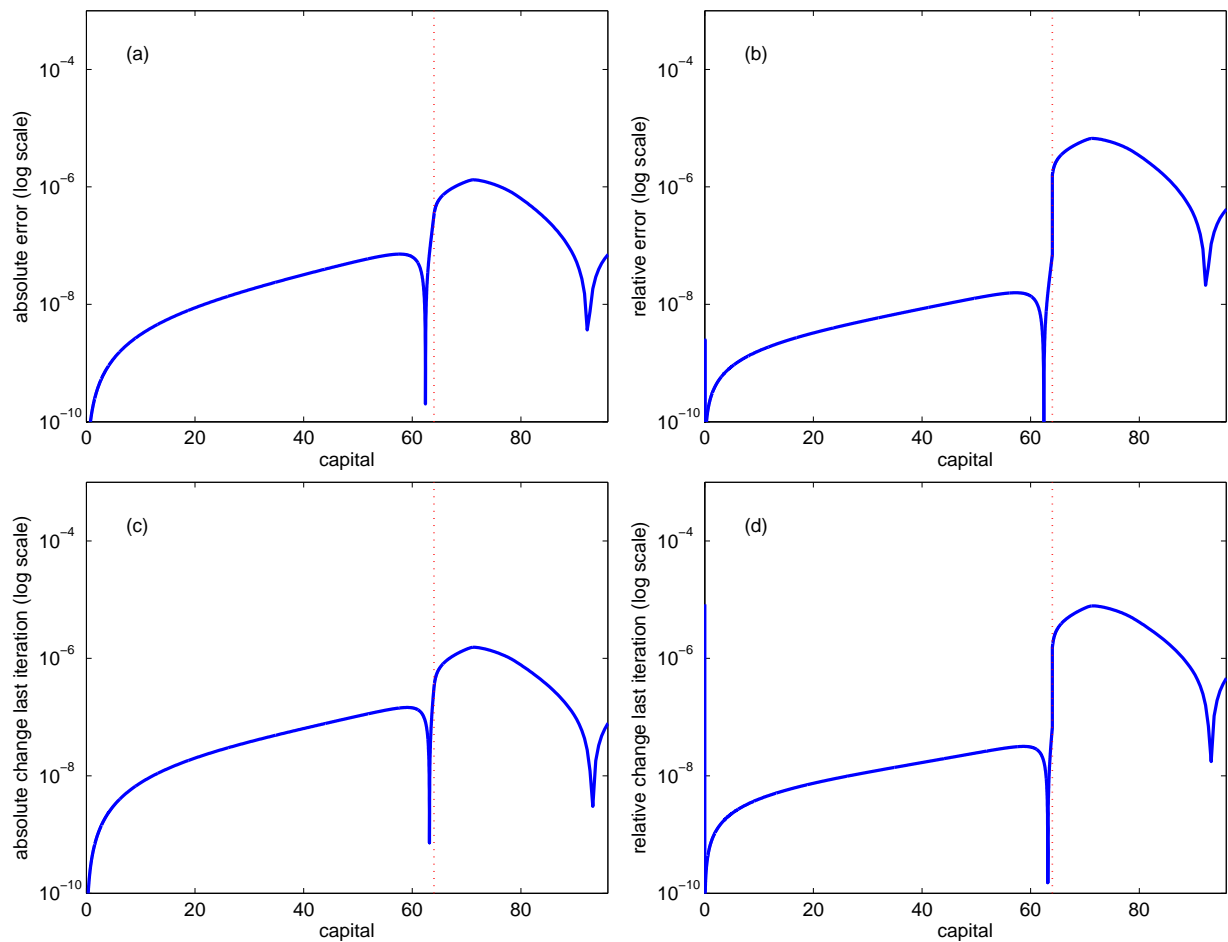
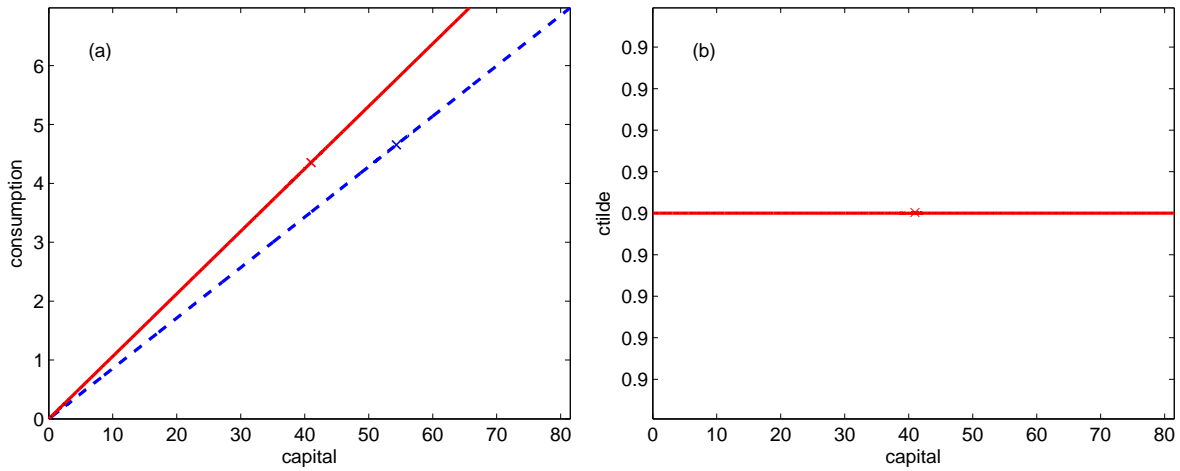


Figure 3: Policy functions and optimal jump in the neoclassical growth model (ii)



Notes: These figures show (a) the optimal policy functions: deterministic (dashed) vs. stochastic (solid) in the neoclassical growth model compared to the analytical benchmark solution (dotted), and (b) the optimal jump as a function of capital for the parameter set 4 from Table 2: $(\alpha, \theta, \delta, \lambda, \gamma, \rho) = (0.5, 0.5, 0.05, 0.2, 0.1, 0.0178)$, which implies a linear policy function.

Figure 4: Absolute and relative error compared to the analytical benchmark solution and to the policy function of the last iteration

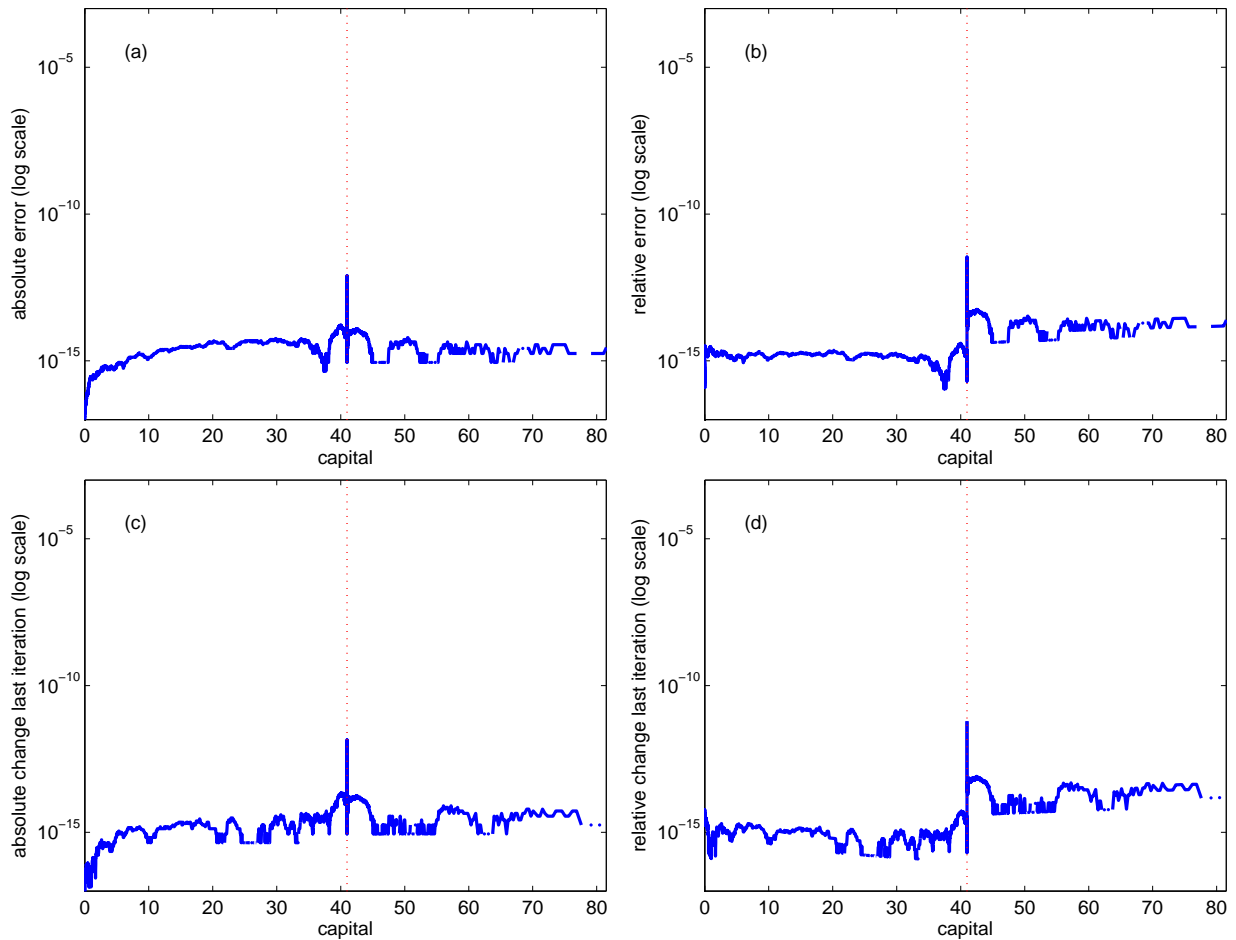
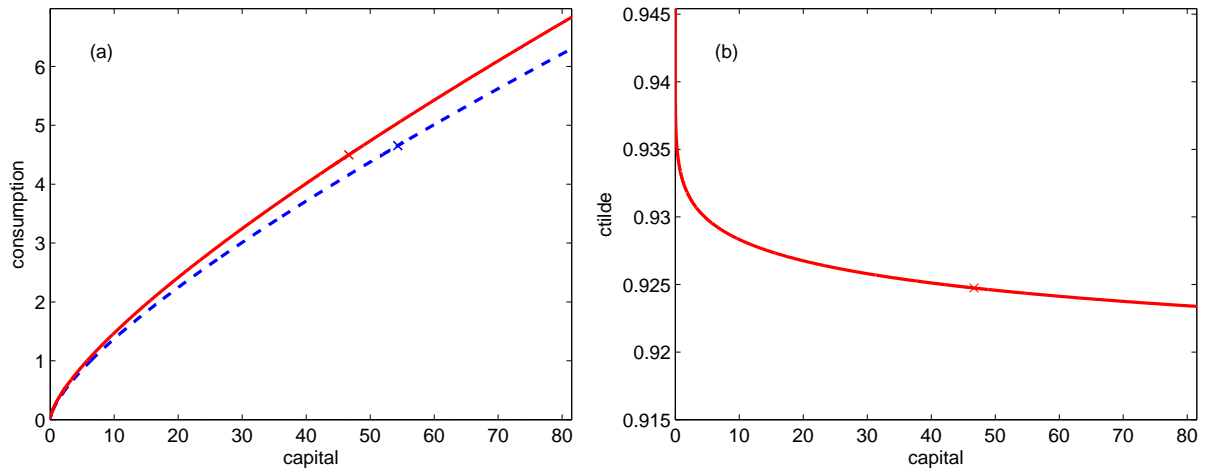
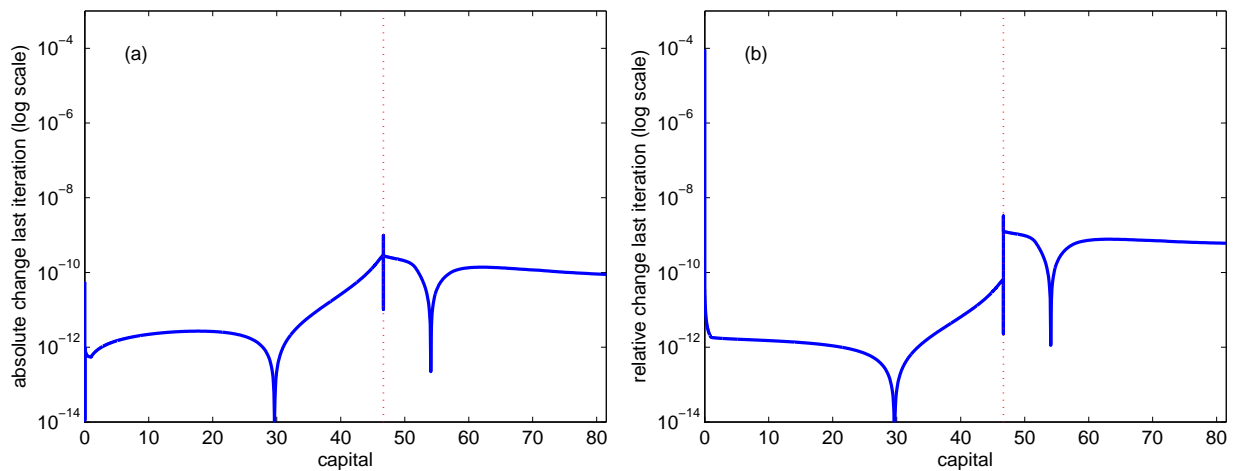


Figure 5: Policy functions and optimal jump in the neoclassical growth model (iii)



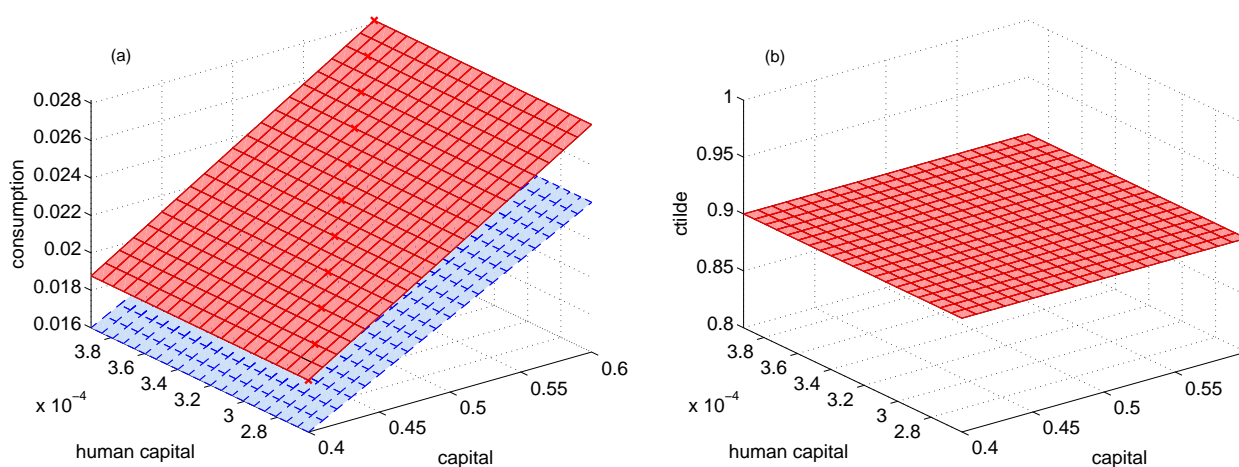
Notes: These figures show (a) the optimal policy functions: deterministic (dashed) vs. stochastic (solid) in the neoclassical growth model (no analytical benchmark solution available), and (b) the optimal jump as a function of capital for the parameter set: $(\alpha, \theta, \delta, \lambda, \gamma, \rho) = (0.5, 1, 0.05, 0.2, 0.1, 0.0178)$.

Figure 6: Absolute and relative error compared to the policy function of the last iteration (no analytical errors available)



B.2 Lucas' model of endogenous growth with disasters

Figure 7: Policy functions and optimal jump for consumption in the Lucas model (1)



Notes: These figures show (a) the optimal policy functions: deterministic (dashed) vs. stochastic (solid) in the Lucas model compared to the analytical benchmark solution (dotted), and (b) the optimal jump as a function of physical capital and human capital for the calibration $(\alpha, \theta, \vartheta, \lambda, \gamma, \rho) = (0.75, 0.75, 0.075, 0.2, 0.1, 0.03)$, which implies a linear policy plane.

Figure 8: Absolute and relative error compared to the analytical benchmark solution and to the policy function of the last iteration

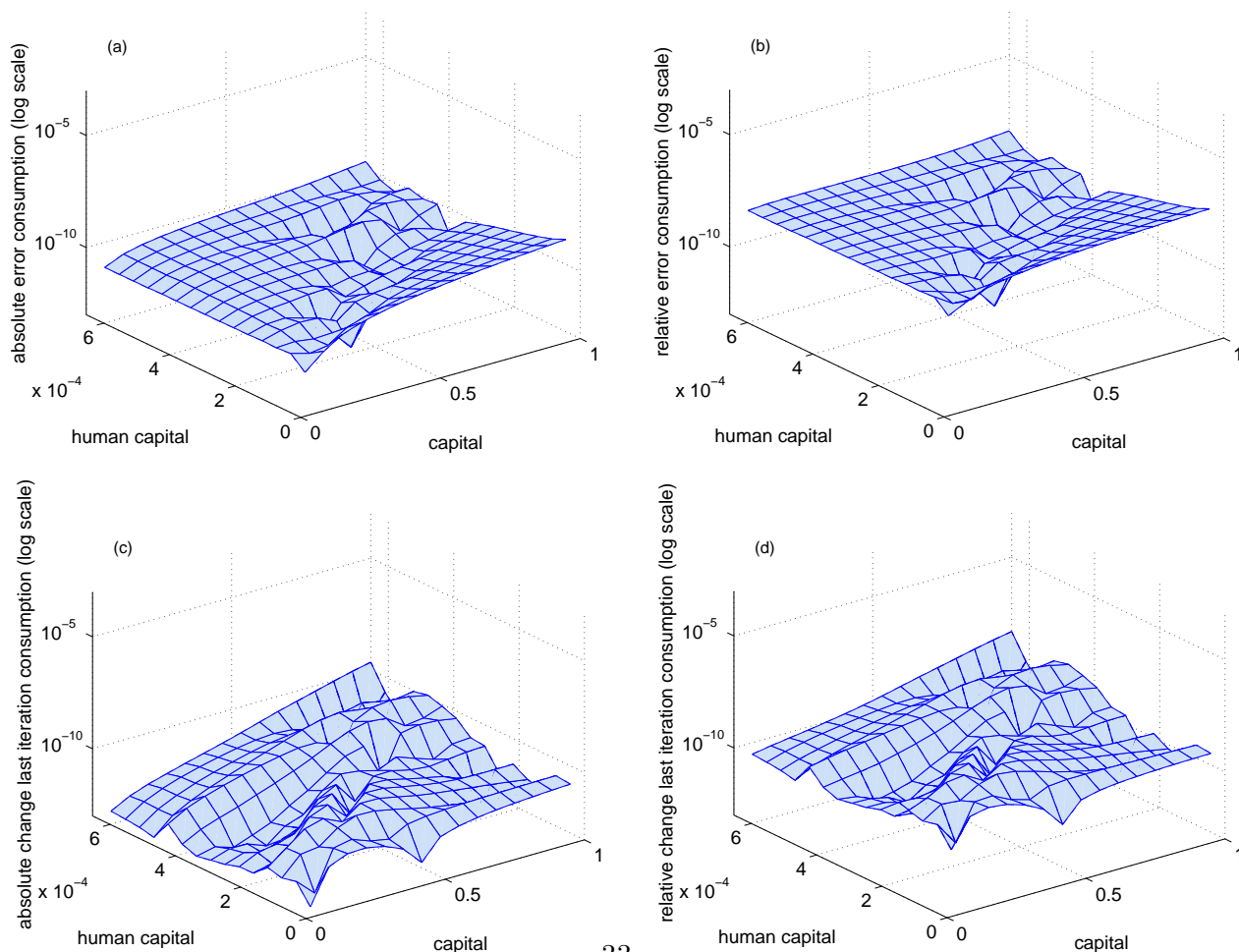
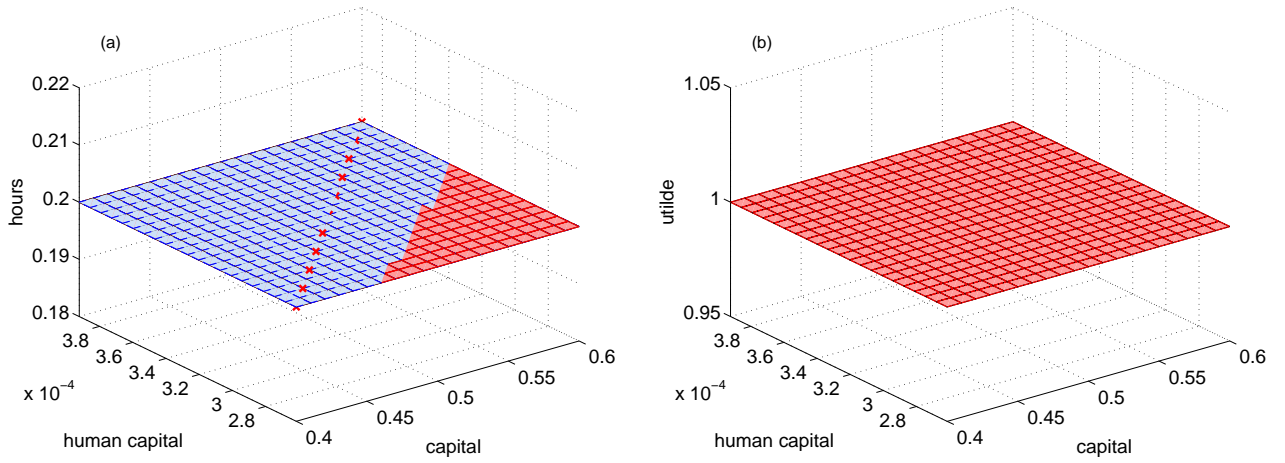


Figure 9: Policy functions and optimal jump for hours in the Lucas model (1)



Notes: These figures show (a) the optimal policy functions: deterministic (dashed) vs. stochastic (solid) in the Lucas model compared to the analytical benchmark solution (dotted), and (b) the optimal jump as a function of physical capital and human capital for the calibration $(\alpha, \theta, \vartheta, \lambda, \gamma, \rho) = (0.75, 0.75, 0.075, 0.2, 0.1, 0.03)$, which implies a linear policy plane.

Figure 10: Absolute and relative error compared to the analytical benchmark solution and to the policy function of the last iteration

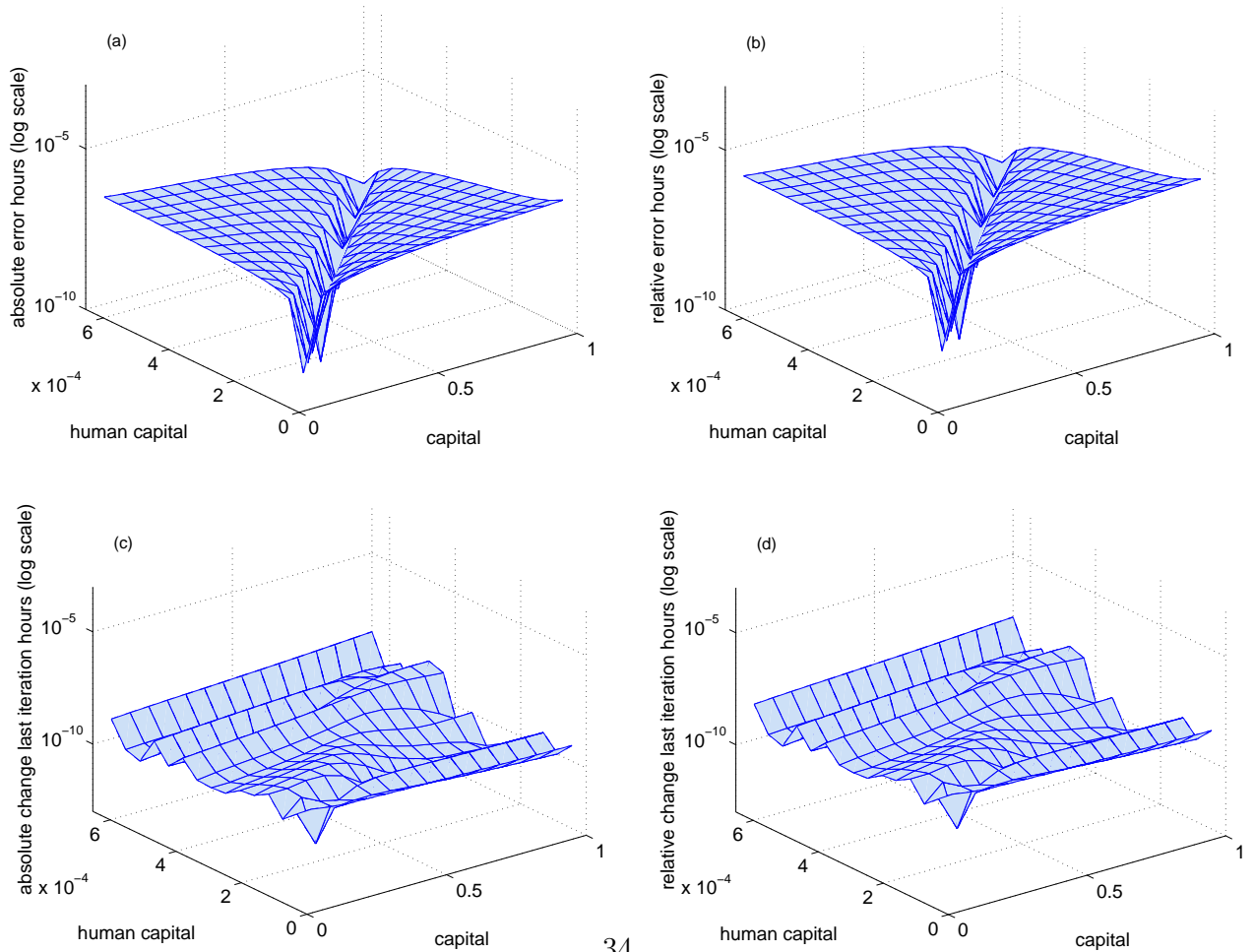
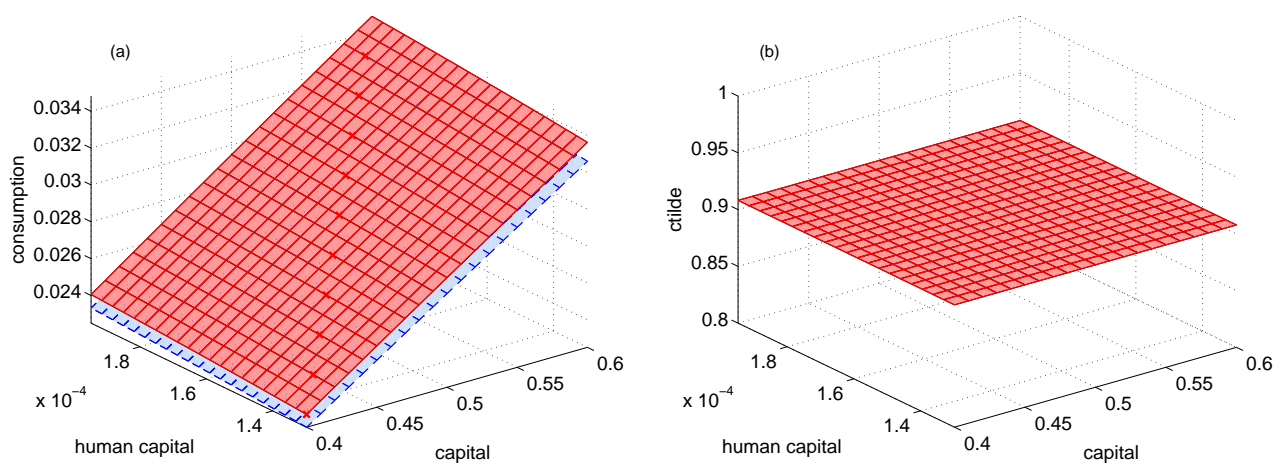


Figure 11: Policy functions and optimal jump for consumption in the Lucas model (2)



Notes: These figures show (a) the optimal policy functions: deterministic (dashed) vs. stochastic (solid) in the Lucas model (no analytical benchmark solution available), and (b) the optimal jump as a function of physical capital and human capital for the calibration $(\alpha, \theta, \vartheta, \lambda, \gamma, \rho) = (0.75, 1, 0.075, 0.2, 0.1, 0.03)$.

Figure 12: Absolute and relative error compared to the policy function of the last iteration (no analytical errors available)

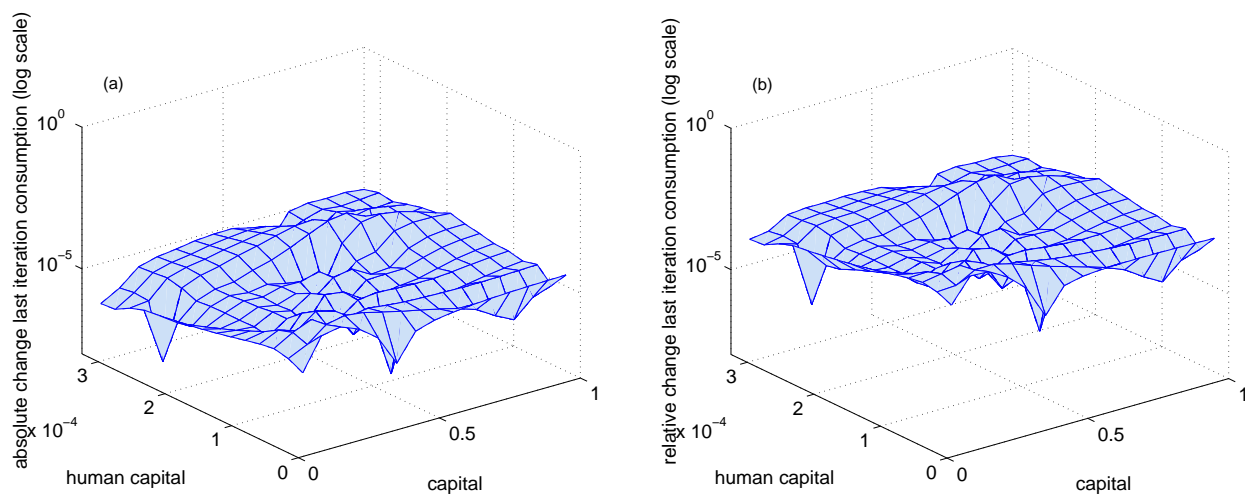
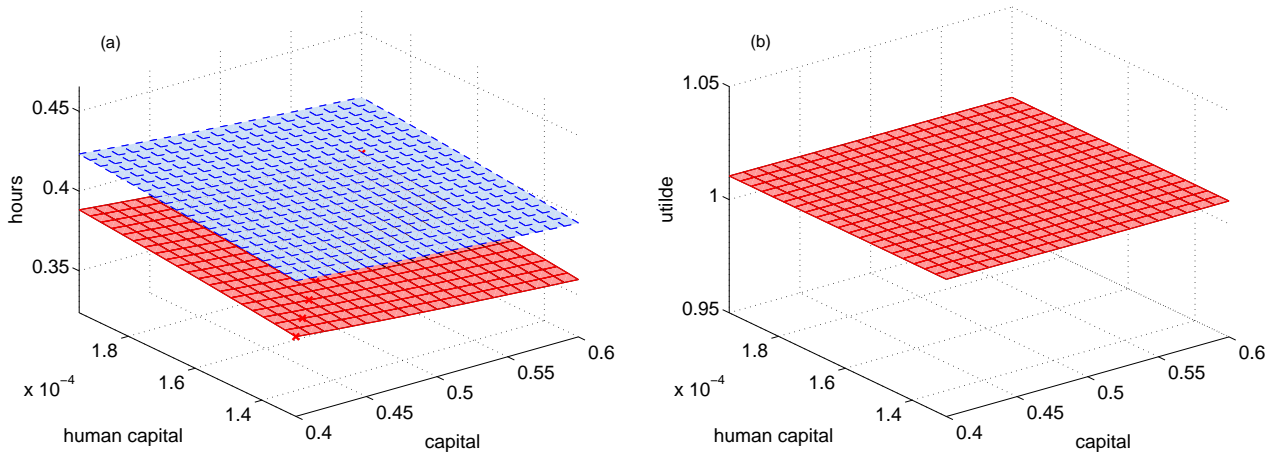


Figure 13: Policy functions and optimal jump for hours in the Lucas model (2)



Notes: These figures show (a) the optimal policy functions: deterministic (dashed) vs. stochastic (solid) in the Lucas model (no analytical benchmark solution available), and (b) the optimal jump as a function of physical capital and human capital for the calibration $(\alpha, \theta, \vartheta, \lambda, \gamma, \rho) = (0.75, 1, 0.075, 0.2, 0.1, 0.03)$.

Figure 14: Absolute and relative error compared to the policy function of the last iteration (no analytical errors available)

